



Spatial Scale of Produced Water Impacts as Indicated by Plume Dynamics

Final Technical Summary

Final Study Report



Spatial Scale of Produced Water Impacts as Indicated by Plume Dynamics

Final Technical Summary

Final Technical Report

Authors

**Sally MacIntyre
Libe Washburn
Principal Investigators**

Prepared under MMS Cooperative
Agreement No. 14-35-0001-30471
by
Southern California Educational Initiative
Marine Science Institute
University of California
Santa Barbara, CA 93106

Disclaimer

This report has been reviewed by the Pacific Outer Continental Shelf Region, Minerals Management Service, U.S. Department of the Interior and approved for publication. The opinions, findings, conclusions, or recommendations in this report are those of the author, and do not necessarily reflect the views and policies of the Minerals Management Service. Mention of trade names or commercial products does not constitute an endorsement or recommendation for use. This report has not been edited for conformity with Minerals Management Service editorial standards.

Table of Contents

FINAL TECHNICAL SUMMARY	1
FINAL TECHNICAL REPORT.....	5
INTRODUCTION	5
METHODS	6
Field Site	6
Instrumentation and Data Processing	6
MODELING OF A BUOYANT PLUME.....	9
Modeling Based on Dimensional Analysis	10
Integral Method	12
FAR FIELD DISPERSION	14
SEASONAL EVOLUTION OF THE WATER COLUMN.....	15
SEASONAL VARIATION OF CURRENTS.....	17
MODEL RESULTS.....	20
Initial Mixing Models.....	20
Far Field Dispersion	24
COMPARISON WITH BIOLOGICAL DATA	27
CONCLUSIONS	29
REFERENCES	30

FINAL TECHNICAL SUMMARY

STUDY TITLE: Southern California Educational Initiative, Study 23: Spatial Scale of Produced Water Impacts as Indicated by Plume Dynamics and Biological Field Assays

REPORT TITLE: Spatial Scale of Produced Water Impacts as Indicated by Plume Dynamics

CONTRACT NUMBER: 14-35-0001-30471

SPONSORING OCS REGION: Pacific

APPLICABLE PLANNING AREA: Southern California

FISCAL YEAR(S) OF PROJECT FUNDING: FY92, FY93

COMPLETION DATE OF THE REPORT: September 1995

COST(S): FY 92 - \$44,331; FY 93 - \$14,000

CUMULATIVE PROJECT COST: \$58,331

PROJECT MANAGER: Russell J. Schmitt

PRINCIPAL INVESTIGATORS: Sally MacIntyre¹, Libe Washburn¹, Craig Osenberg²

AFFILIATION: ¹University of California, Santa Barbara, ²University of Florida

ADDRESS: ¹Marine Science Institute, University of California, Santa Barbara, CA 93106;
²Department of Zoology, University of Florida, Gainesville, FL 32611

KEY WORDS: Produced water; plume; near and far field dispersion; dilution; ambient stratification; mussels; diffuser; modeling; toxicity

BACKGROUND: Previous SCEI studies have demonstrated significant deleterious effects of produced water on marine organisms. Our study was motivated by years of discharge of produced water into the Santa Barbara Channel via a diffuser extending 300 m offshore from Carpinteria, CA. Densities of several infaunal groups, growth rates of mussels, and settlement and metamorphosis of abalone larvae were negatively impacted by the produced water. However, the biological experiments designed to assess the effects of the plume were limited to alongshore transects up to 1000 m from the diffuser. Our goal was to provide a more complete assessment of the spatial extent of produced water by characterizing the near and far-field dispersion of the buoyant plume produced by the diffuser. Coupling the results of this physical study with the results of the biological experiments will permit a better assessment of the area where organisms were negatively impacted by the plume.

OBJECTIVES: 1) To determine the seasonal stratification and current structure in coastal waters near Carpinteria, California; 2) To model the height of rise, thickness and dilution of the plume of produced water in these coastal waters; 3) To determine the spatial extent of the plume of produced water; 4) To compare the results of plume modeling with bio-assays undertaken by other investigators which assessed changes in viability and growth rates of organisms in the study area.

DESCRIPTION: Because a buoyant plume rises in the water column and its dilution depends on ambient stratification and current structure, we undertook a year long study to characterize the stratification and current velocities of the coastal waters near Carpinteria, California. Our study included profiles taken about every two weeks (weather permitting) from 28 July 1992 to 3 January 1994 of conductivity, temperature and depth (CTD) at the diffuser site as well as profiles 100 m inshore, offshore and up and down coast of the diffuser. We used these data to determine the temperature, salinity and density stratification of the water column as well as the buoyancy of the plume relative to the water column. In addition, we deployed current meters 1 m and 5 m above the bottom for nearly a year. Our sampling included times when the water column was gaining and losing heat as well as times when high rainfall from storms.

We modeled the plume's height of rise, thickness, and dilution close to the diffuser using as input the data we collected on ambient stratification and current speeds. We used two well known models, the Morton-Taylor-Turner (MTT) model which is an integral model, and the Roberts-Snyder-Baumgartner (RSB) model which is based on dimensional analysis. We used low (0.01 ms^{-1}) and moderate (0.1 ms^{-1}) current speeds as input to the RSB model.

We used the combination of visitation diagrams and relative dilution diagrams to describe the spatial extent of the plume in the far field. The visitation diagrams assess the frequency of the plume waters occurring in any location up to 2 km up or down coast from the diffuser, inshore of the diffuser and 1 km offshore from the diffuser. The dilution diagrams indicate the additional dilution of the plume as it moves away from the diffuser due to ambient turbulence. We used these data on the plume's location in the far field to further interpret the biological field data.

SIGNIFICANT RESULTS AND CONCLUSIONS: The water column was stratified and the plume's height of rise was therefore limited due to heating in spring and summer and due to freshwater inputs during winter storms. Thermal stratification occurred from April through September and salinity stratification occurred during part of January and part of February and March 1993. The limitation of the height of rise due to thermal stratification is predictable since it is a result of the annual heating cycle, but the limitation in winter is less predictable because it depends on freshwater inputs which vary due to storm frequency and intensity. The plume is up to an order of magnitude more concentrated in the near-field when it is restricted to the lower third of the water column during periods of stratification than when it extends through the entire water column.

Large diurnal fluctuations in current velocity occur due to diurnal and semi-diurnal tidal forcing. Current speeds ranged from 0 to 0.2 ms^{-1} 5 m above the bottom and ranged from 0 to 0.1 ms^{-1} 1 m off the bottom. Five m above the bottom, current directions tended to be alongshore with only intermittent episodes of cross-shore flow. Currents moved in all directions 1 m above the bottom, although less flow occurred onshore. The current velocities 5 m above the bottom are likely to be representative of currents in the upper part of the water column when the water column is unstratified. Produced water would be swept alongshore in both directions. In contrast, during stratified periods, the movement of the plume is better characterized by the currents measured 1 m from the bottom. In this case, the plume will be

carried in all directions. Due to the lesser dilution in the near-field and the assumption of similar turbulent diffusion, concentrations will be higher over a larger area.

Previous experimental outplantings of mussels indicated that effects of the plume could be noted as far as 0.5 km and perhaps as far as 1 km from the diffuser. Waters with a similar dilution to that at the outplantings at 0.5 km were restricted to a band 0.8 km to the west, 0.5 km to the east, and 0.15 km inshore and offshore of the diffuser based on the current velocities 1 m above the bottom. It would have been somewhat elliptical in shape, extending 1 km offshore, 0.7 km west and 0.5 to 1.1 km east of the diffuser.

The plume affected growth rates and production of gonadal mass in the mussels, both of which depend on integrated exposure time to produced water. However, experiments by other investigators with planktonic larvae and other invertebrates indicated that short exposures to produced water could affect fertilization success, larval survivorship and settlement, and relative viability. Our calculations of visitation frequency, the length of time that the plume spent at any given location, indicated that the plume could reside for hours at distances of several km outside the region causing integrated effects on mussels. These sporadic excursions of plume water intermittently will affect survivorship of larvae of a variety of species up to several km from the diffuser.

STUDY PRODUCTS:

Washburn, L., S. Stone, and S. MacIntyre. 1999. Dispersion of produced water in a coastal environment and its biological implications. *Continental Shelf Research* **19**:57-78.

Stone, Shannon. 1995. *The Seasonal Variation of a Buoyant Plume in a Stratified Environment*. Master of Science Theses. University of California, Santa Barbara, CA. 45 pp.

MacIntyre, S., A.L. Alldredge, and C.G. Gotschalk. 1995. Accumulation of marine snow at density discontinuities in the water column. *Limnol. Oceanogr.* **40**:449-468.

Stone, S., L. Washburn, and S. MacIntyre. 1994. Seasonal variations of a buoyant plume in a stratified environment. Ocean Science Meeting, American Geophysical Union. San Diego, CA. [abstract]

Stone, S., L. Washburn, and S. MacIntyre. 1994. Seasonal variations of a buoyant plume in a stratified environment. UC Toxic Substances Research and Teaching Program Annual Symposium. San Diego, CA. [abstract]

Stone, S., L. Washburn, and S. MacIntyre. 1994. Seasonal variations of a buoyant plume in a stratified environment. Annual Meeting of The Oceanography Society, Newport, R.I. [abstract]

FINAL STUDY REPORT

INTRODUCTION

Offshore oil production has increased dramatically in recent years as oil deposits on land have become depleted. Because many oil deposits reside in or around natural groundwater aquifers, large amounts of water are extracted along with oil in the drilling process. In addition, new drilling techniques pump water into oil wells to increase pressure, causing greater oil extraction, but also result in large quantities of water being removed along with the oil. This so called “produced water” is separated in the production process and then is disposed of, sometimes into nearshore waters. Produced water contains many contaminants including hydrocarbons, heavy metals, and chemical additives, such as corrosion inhibitors to prevent damage to refinery equipment (Higashi *et al.*, 1992). Following separation from oil, produced water is generally discharged directly into the marine environment through ocean outfalls. It is one of the largest sources of pollution associated with oil production (Krause, 1993). Until recently it was believed that the largest impact of produced water resulted from solids released with the discharge. These solids quickly settle out of the buoyant produced water plume and limit the spatial impact of solid components in the produced water.

However, recent studies show broad spatial impacts of produced water in the marine environment (Krause, 1993, Krause *et al.*, 1992, Osenberg *et al.*, 1992 and Raimondi and Schmitt, 1992). In a field study off the coast of Carpinteria, California, Osenberg *et al.* (1992) found a decrease in growth rates along with a decline in the general condition and tissue production of mussels at distances up to 500 m to 1000 m from a produced water diffuser. At the same field site, Raimondi and Schmitt (1992) found that the settling rates of red abalone were adversely affected by exposure to produced water. They reported decreasing viability, defined as the fraction of larvae that become adults, of red abalone larvae with increasing proximity to the diffuser. Krause (1993) exposed adult purple sea urchins to varying concentrations of produced water and found no difference in survivorship. However, as adults broadcast eggs and sperm into the water column, the success of reproductive fertilization of the purple sea urchin was reduced for dilutions of up to 1,000,000:1. Krause (1993) developed a one-dimensional plume profile at the diffuser site by exposing purple sea urchins to samples of seawater collected at increasing distances west (upcoast) of the diffuser and then, using reproductive success, inferred the concentration of the produced water in the sample. This method of determining the toxicity provides a useful means of observing the effects of produced waters in the environment (Krause, 1993). While these studies are valuable, they are limited in spatial and temporal scales (spatial scales less than 1000 m and time scales on the order of 10 days) and cannot predict the extent or fate of the produced water over a seasonal or yearly cycle. Moreover, they assume a uniform, unvarying water column. To determine the biological impact of produced water over more extensive space and time scales, direct observation and modeling of produced water dispersion is required (Keough and Black, 1993).

METHODS

Field Site

The produced water diffuser is located about 300 m off the coast of the city of Carpinteria, California (34° 23' N, 119° 30' W) 300 m to the west of the Casitas Pier (**Figure 1**). In this location, the coast runs east-west with the Pacific Ocean to the south. The diffuser section through which the produced water is released is 30 m in length and lies on the sea floor at a depth of 12 m. The diffuser consists of 10 T-ports that rise off of a central pipe that is 0.20 m in diameter. Each T-port riser discharges effluent horizontally into the water column through two oppositely-directed nozzles, each 10 cm in diameter. The sea floor near the diffuser has a gently sloping sandy bottom with isobaths oriented parallel to the coastline. The coastline itself runs at about a 115° angle with respect to true north, and the shelf break (200 m depth) lies 3.25 km to the southwest of the diffuser. The Casitas Pier, operated by Chevron Inc., is located 300 m east of the diffuser and extends 200 m from the beach; this pier is the only flow impediment near the diffuser. Roughly 2 km west of the diffuser is the discharge channel of the Carpinteria slough. Several creeks drain the watershed surrounding the city of Carpinteria and empty into the local waters (**Figure 1**).

Daily totals of rainfall within the drainage basin emptying into our study site show the importance of winter rains in this area (**Figure 2**). During our study, the largest accumulations occurred due to storms in late December 1992 through mid-January 1993, the second half of February 1993, and in late March 1993 (**Figure 2**). Rainfall is highly intermittent on both seasonal and annual time scales.

Instrumentation and Data Processing

Profiles of temperature, conductivity and pressure were taken every two weeks, weather permitting, from July 29, 1992 to January 4, 1994 using a conductivity, temperature, depth profiler CTD (Sea Cat SBE 19 manufactured by Sea-Bird Electronics Inc., Bellevue WA). Profiles were made at five nominal locations: over the diffuser, 100 m to the east, 100 m to the west, 100 m inshore and 100 m offshore of the diffuser (**Figure 1**).

The CTD used for this field study was calibrated in March of 1992 and again in January 1994 with only minor differences in calibration coefficients. The pressure sensor for the CTD is a 500 psi (~ 340 dbar) Senso-Metrics SP-91 strain gauge sensor. Temperature is sensed by a glass encased thermister, and a three electrode conductivity sensor measures the conductivity of seawater supplied by a small submersible pump. The measuring range, accuracy and resolution of the CTD are presented in **Table 1**.

Table 1. Measuring range, accuracy and resolution of the SEACAT SBE 19 CTD.

	Measuring Range	Accuracy	Resolution
Temperature	-5 to 35°C	0.01°C/6 months	0.001°C
Conductivity	0 to 7 S/m	0.001 S/m /month	0.0001 S/m
Pressure	0 to 500 psi	0.5% of full range	0.03% of full range

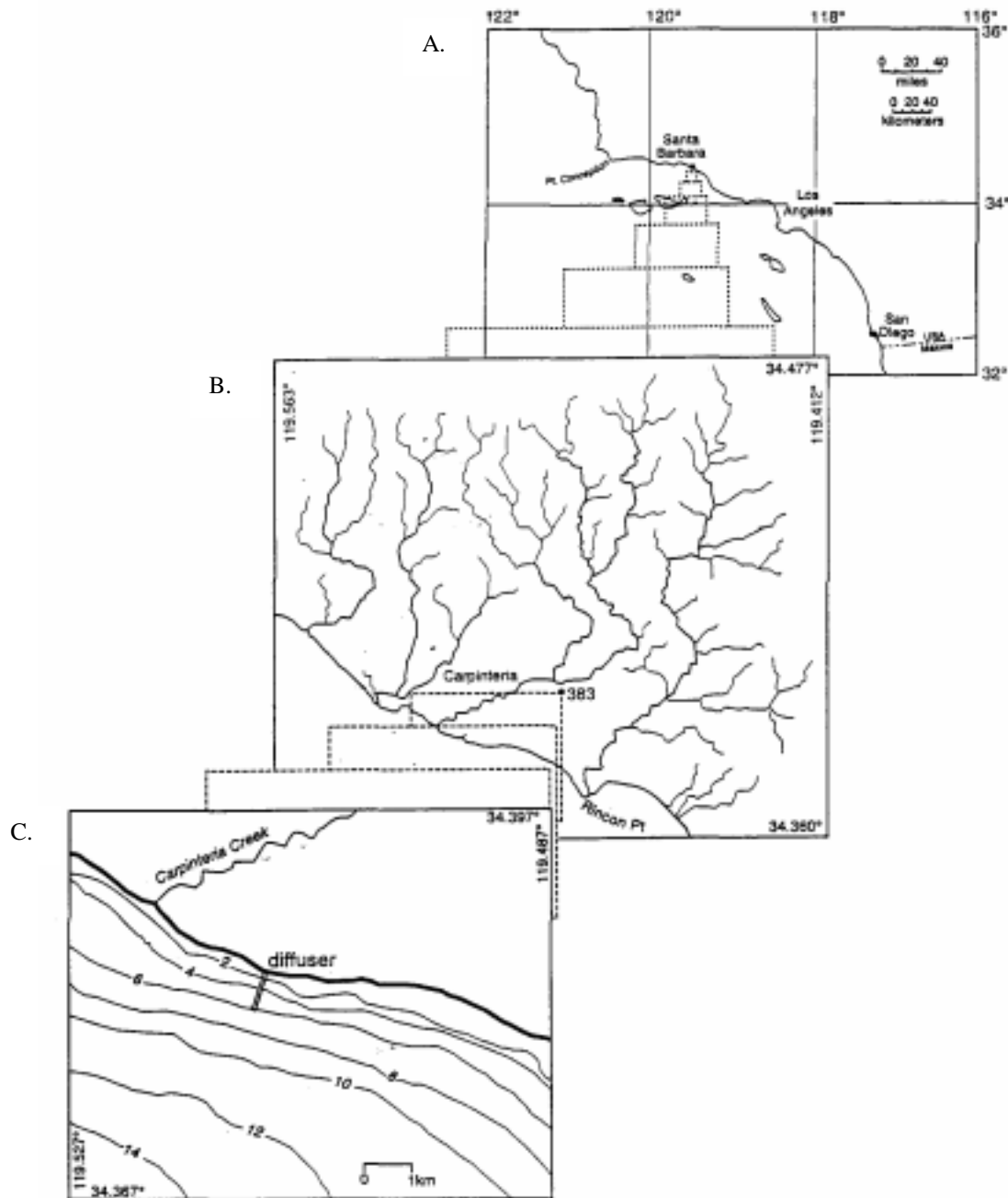


Figure 1. Map of the study area. A. Carpinteria is located in southern California approximately 80 miles north of Los Angeles and 5 miles southeast of Santa Barbara. The coastline around the city of Carpinteria runs east-west with an angle of 115 degrees with respect to true north. B. Creeks draining the watershed in the vicinity of the field site. C. Location of the diffuser in 12 m of water approximately 300 m from shore.

Because of differing response times, temperature and conductivity data were smoothed using a low pass filter with a time constant of 0.10 seconds. The conductivity and temperature sensors were not at exactly the same depth, and to account for the pumping time of the conductivity sensor, the conductivity signal was shifted by -0.25 seconds relative to the pressure signal. Similarly, the temperature signal was shifted by 0.40 seconds relative to the pressure signal. Variations in profiling speed occurred as the CTD was lowered by hand from a small boat. All data obtained with vertical profiling speeds of less than 0.20 m s^{-1} were discarded. Remaining data were divided into 0.5 meter depth bins for down-casts only, and all data points in each bin were averaged to give a single value for each bin. Finally,

conductivity, temperature and pressure data were used to compute salinity and density using the method developed by Fofonoff and Millard (1983). The Seabird SBE 19 CTD is unable to record data in the upper 0.5 m of the water column due to instrument configuration and therefore data from the upper 0.5m of the water column is unavailable. Due to daily tidal differences, the observed water column depth above the diffuser varied from 10.5 to 12.5 m.

Rainfall Data: Casitas Pass Road

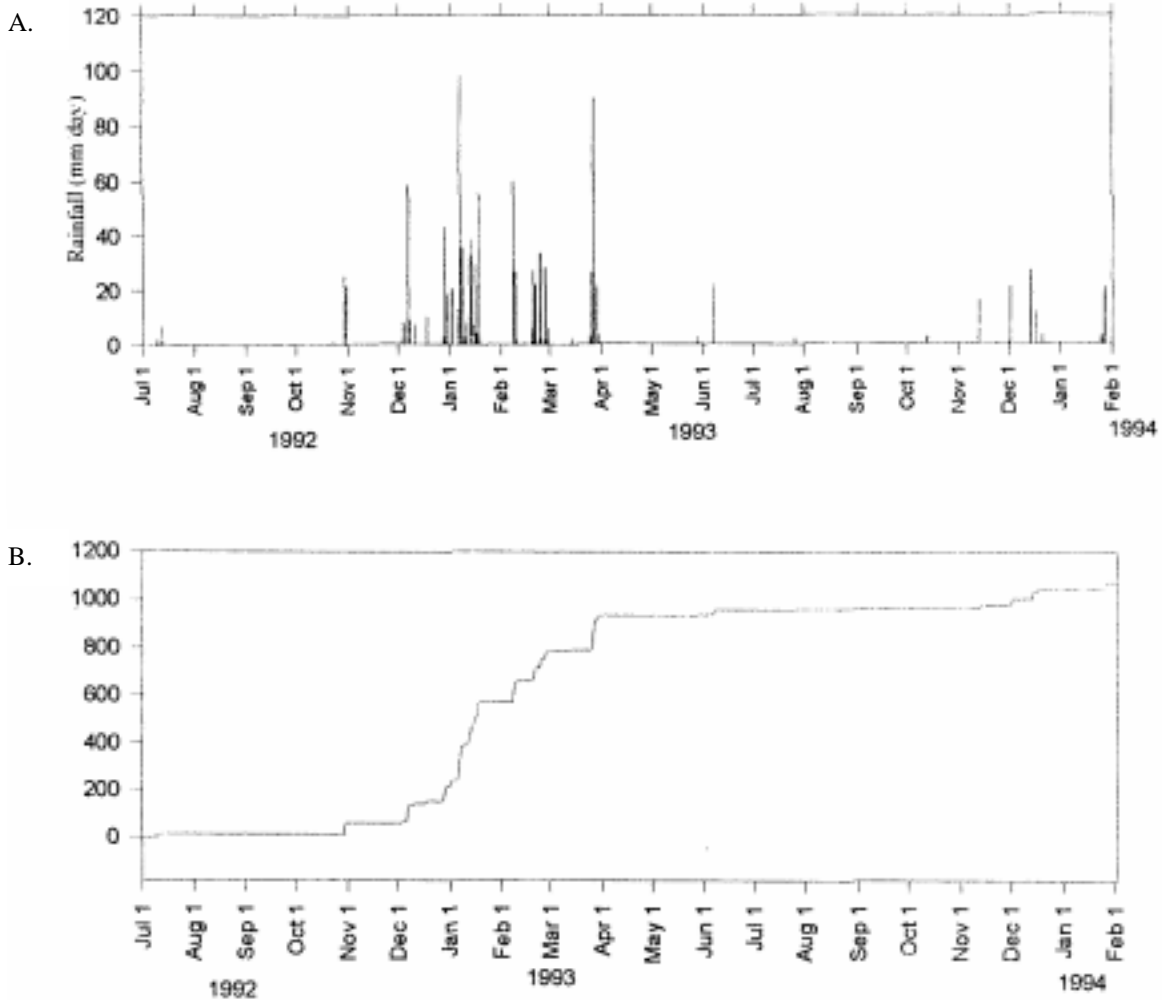


Figure 2. Rainfall totals in the catchment draining into the Carpinteria slough from July 1, 1992 to February 1, 1993. A. Daily rainfall (mm/day). B. Cumulative rainfall total (mm).

Current magnitude and direction were measured by mooring two electromagnetic current meters (Model S4, manufactured by Interocean Inc., San Diego, CA) 25 m to the west of the diffuser. The first current meter was moored 5 m from the bottom (approximately 6 m from the sea surface), and the second S4 current meter was moored 1m from the sea floor. Two different pairs of S4 current meters were used to collect data. The first pair of current meters was deployed from December 20, 1992 to April 16, 1993 and the second pair from July 13, 1993 until January 3, 1994. For all deployments the S4 current meters were configured to

collect 2 minute vector averages of currents and record a single vector average every 20 minutes.

In its operation, the S4 current meter creates an electromagnetic field in the seawater surrounding the current meter. As seawater flows past, a voltage is produced because it is a conductor and it is flowing through an electromagnetic field. The resulting voltage is sensed by two pairs of electrodes on the side of the current meter. The differences in voltages sensed by the electrode pairs determine the current direction (measured in the horizontal plane), while the magnitude of the voltage determines the current speed. The current meters have a sensing range of 0-350 cm s^{-1} and an accuracy of $\pm 0.03 \text{ cm s}^{-1}$ (Interocean Inc., 1990). Due to their spherical shapes and surface structure, flow over the current meters is not fully turbulent until about 1 cm s^{-1} . This transition causes the current meters to become inaccurate for current speeds around 1 cm s^{-1} . These inaccuracies in the S4 signals were observable as distinct peaks at 0, 90, 180 and 270 degrees in histograms of current direction. To remove these peaks, we omitted currents under 2 cm s^{-1} from the histograms.

MODELING OF A BUOYANT PLUME

Two general methods are used to model the behavior of buoyant jets. The simplest method is dimensional analysis in which scaling laws are used to determine the non-dimensional parameters which characterize a buoyant jet. However, dimensional analysis methods are generally applicable only for receiving fluids that have uniform or linear density profiles, a situation that seldom occurs at our field site. The other method, the integral method, uses the equations of motion for fluids and allows realistic, non-linear density stratification to be accounted for in determining plume characteristics. Both methods are used in this study to characterize the initial mixing of the produced water plume due to buoyancy and momentum fluxes. Both methods use a cylindrical coordinate system; r and z give radial and vertical directions (**Figure 3**) with positive z upwards.

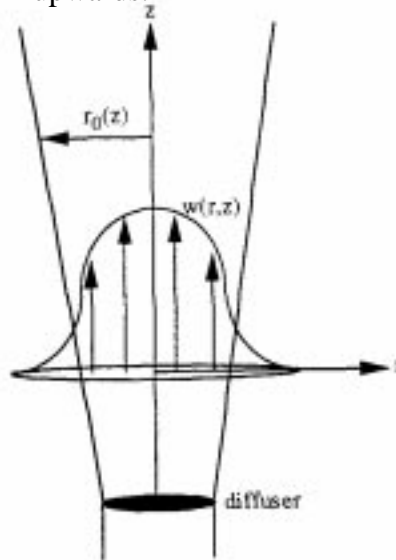


Figure 3. Schematic diagram of a buoyant jet released from a point source. Vertical and radial direction are denoted by z and r , with $r_0(z)$ being the distance at which the vertical velocity (w) is $1/e$ the centerline value. The vertical velocity profile and concentration profiles are assumed Gaussian at all heights (z).

Modeling Based on Dimensional Analysis

In the dimensional analysis method, the critical parameters for modeling plume characteristics are: fluxes of volume (q), momentum (m) and buoyancy (b) per unit length of diffuser as well as the buoyancy frequency N to characterize the stability of the water column, the produced water effluent and the diffuser. The variables are (c.f. Fischer *et al.* 1979),
 volume flux per unit length

$$q = Q / L, \quad (1)$$

momentum flux per unit length

$$m = u_j q, \quad (2)$$

buoyancy flux per unit length

$$b = g_o' q, \quad (3)$$

and buoyancy frequency

$$N = \left[\left(\frac{g}{\rho_a} \right) \left(\frac{d\rho}{dz} \right) \right]^{\frac{1}{2}}. \quad (4)$$

Here Q is the total volume flux of discharge, L is the diffuser length, u_j is the velocity of the effluent as it leaves the diffuser and g_o' is the reduced gravitational acceleration

$$g_o' = g \frac{(\rho_a - \rho)}{\rho_o} \quad (5)$$

A Froude number $F_r = \frac{u^3}{b}$, based on the ambient current velocity u, is defined to compare the rate of potential energy input to the water column with the flux of kinetic energy due to currents. High values of F_r lead to a diffuse plume as the ambient currents disperse and mix the effluent. Low values of F_r result in a more concentrated plume because ambient dispersion and mixing processes are weaker.

Given these parameters, the main geometrical characteristics of the plume can be expressed by

$$h_e, z_e, h_m = f(q, b, m, s, u, N) \quad (6)$$

where h_e height of the top of the wastefield, z_e is the wastefield thickness, h_m is the height of maximum pollutant concentration, and s is the distance between ports (**Figure 4**). Roberts, Snyder and Baumgartner (1989 a,b,c) performed experiments on plume dispersal in stratified water columns to determine the coefficients that give the empirical form of these equations. The resulting Roberts, Snyder and Baumgartner (RSB) model is based on these equations and is used to characterize the produced water plume. The RSB model assumes that the density profile is linear over the rise height, which allows a solution to these equations for the following quantities:

(1) non-dimensional initial dilution,

$$\frac{S_m q N}{b^{2/3}} = 2.19 F_r^{1/6} - 0.52 \quad (7)$$

(2) non-dimensional height of the top of the wastefield,

$$\frac{h_c}{l_b} = 2.5 F_r^{1/6} \quad (8)$$

where $l_b = \frac{b^{1/3}}{N}$ is a length scale where buoyancy effects begin to dominate momentum effects and S_m is the initial dilution of the plume. Baumgartner *et al.* (1994) argue that the linear stratification assumption works well for nonlinear stratification and produces conservative estimates of initial dilution. Due to the variation in the volume of water pumped from oil wells, the volume flux, temperature, and composition of the discharged produced water varied on a daily basis. The values reported in **Table 2** were used for the design of the produced water diffuser and in our calculations.

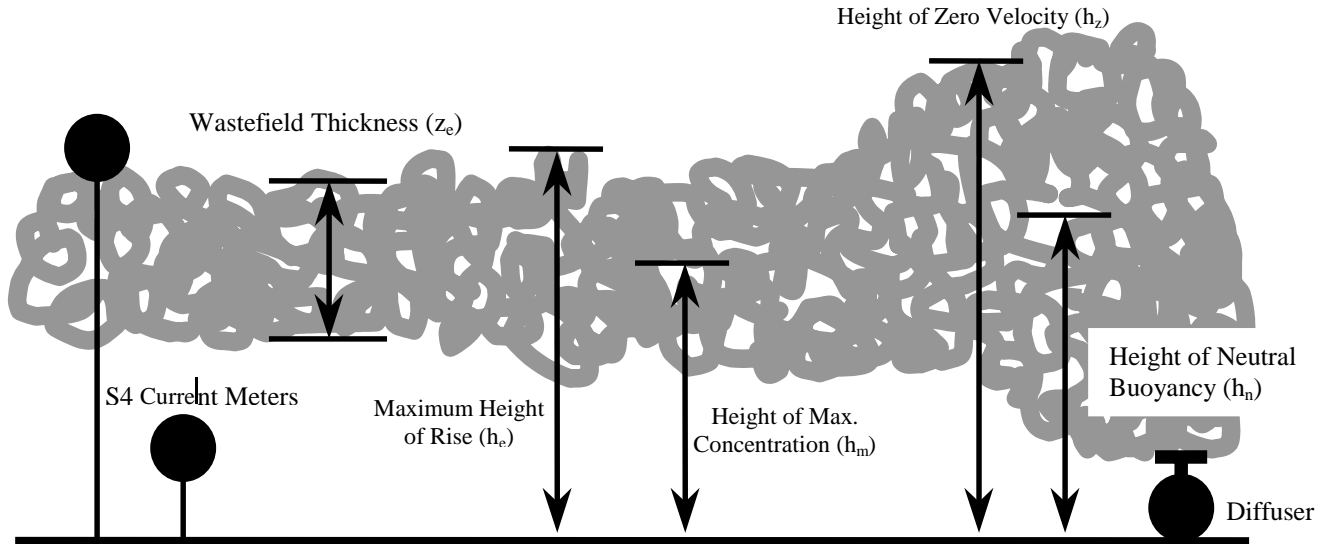


Figure 4. Side View of Plume. The RSB model predicts the maximum height of rise (h_c) of the plume, the height of maximum pollutant concentration (h_m) in the wastefield and the wastefield thickness (z_e). MTT model predicts the height in the water column at which the density difference between the plume and ambient waters is zero (h_n), the height when the plume has no momentum (h_z) and the wastefield thickness (z_e). Two current meters were deployed 25 m to the west of the diffuser at 1 m and 5 m from the bottom.

Table 2. Produced Water Characteristics reported by Chevron Inc. (personal communication from William Ford, 1994).

Temperature	21°C
Density	1011.5 kg/m ³
Discharge Rate	750 gpm

The values of q , m and b (b) are for a single diffuser port and allow calculation of the parameters used to initialize the RSB model.

Table 3. Initial Parameters for Dimensionless Analysis

volume flux	q	$3.94e^{-3} \text{ m}^2 \text{ s}^{-1}$
momentum flux	m	$1.186e^{-3} \text{ m}^3 \text{ s}^{-2}$
buoyancy flux	b	$4.718e^{-4} \text{ m}^3 \text{ s}^{-3}$

To summarize, the RSB model uses stratification, initial buoyancy and volume fluxes along with ambient current velocity to predict initial dilution of the effluent, the height of the top of the wastefield and the wastefield thickness (**Figure 4**). The RSB model does not predict the horizontal extent of the wastefield or the pollutant concentration in the far field.

Integral Method

Several assumptions are needed to find solutions to the equations of fluid motion for buoyant turbulent jets. The primary assumptions are: the fluid is incompressible, the motion induced by the buoyant jet is dominant, and the buoyant jet is fully turbulent. The three fundamental equations governing a radially symmetric buoyant plume flow (Morton *et al.*, 1956), are:

conservation of mass

$$\frac{\partial w}{\partial z} + \frac{1}{r} \frac{\partial (ru)}{\partial r} = 0, \quad (9)$$

conservation of vertical momentum

$$w \frac{\partial w}{\partial z} + u \frac{\partial w}{\partial r} = g \frac{(\rho_a - \rho)}{\rho_o} - \frac{1}{r} \frac{\partial (r \overline{w'u'})}{\partial r}, \quad (10)$$

and conservation of tracer concentration

$$w \frac{\partial C}{\partial z} + u \frac{\partial C}{\partial r} = -\frac{1}{r} \frac{\partial (r u' C')}{\partial r}, \quad (11)$$

where the coordinates r and z give the radial and vertical directions with positive z upwards (**Figure 3**). Velocities in the vertical and horizontal directions are given by w and u respectively, ρ is density in the plume, and ρ_a is the density of the ambient fluid. A reference density ρ_o , is defined as the ambient density at the level of discharge (Morton *et al.*, 1956, Fischer *et al.*, 1979 and Turner, 1986). The concentration of a tracer C such as buoyancy is,

$$C = \frac{(\rho - \rho_a)}{\rho_o} \quad (12)$$

The primes (') in (10) and (11) indicate turbulent fluctuating components of a given quantity and an overbar denotes a time average.

Equation (10), the conservation of vertical momentum, requires that all sources of vertical momentum originate at the diffuser during plume discharge or are induced by density differences between the plume and the ambient fluid. Equation (11), the conservation of tracer concentration, states that the only source of tracer is the discharge from the diffuser, and that this tracer is neither created or destroyed in the plume. In the integral method, these equations (9-11) are simplified and integrated using the method developed by Morton *et al.* (1956).

The diffuser at the Carpinteria site discharges produced water horizontally through the T-ports and the resulting individual plumes must turn upwards. Thus the discharge is initially a jet, but quickly evolves into a buoyant plume. As the physics of the transition from a horizontally discharged buoyant jet to a vertical buoyant plume are poorly understood (Angelidis and Kotsovinos 1994), a simple one-dimensional plume model for a point source of buoyancy in a stratified water column is used (Morton *et al.* 1956). A common assumption in the literature is to treat the series of point sources in a multiport diffuser as a line source of buoyancy (c.f. Wu, 1994, Wu *et al.*, 1993 and Roberts *et al.*, 1989 a,b,c). However, due to the shallow depth of discharge and the spacing of the T-ports at the diffuser, adjacent plumes do not merge for over half their rise height and modeling this diffuser as a line source would inaccurately describe the physics of mixing in the plume. Therefore the discharge from each diffuser port was modeled as a separate buoyant plume.

In order to solve the equations of motion using the integral method, several additional assumptions must be made. First, the velocity, density and concentration profiles are assumed to be similar and have a Gaussian shape at all heights. Second, the entrainment assumption (Morton *et al.*, 1956, reviewed by Kotsovinos and List, 1977, Fischer *et al.*, 1979 and Turner, 1986) relates the rate of mixing of ambient water into the plume (entrainment) at a given height to the centerline velocity of the plume (see Eq. (13)) at that height.

The entrainment relation may be expressed as,

$$\frac{d\mu}{dz} = 2\pi r_o \alpha w \quad (13)$$

where r_o is as the plume radius at which the magnitude of the velocity of the plume decreases to 1/e of its centerline value (**Figure 4**). The entrainment coefficient, α , ($\alpha=0.083$ Turner, 1986) is the constant of proportionality in the entrainment relation, and μ is the volume flux of the plume. Finally, variations in density are assumed small compared to the reference density (the Boussinesq approximation). Using these assumptions, Eqs.(9), (10) and (11) simplify to:

conservation of mass

$$\frac{d[\pi r_o^2 w]}{dz} = 2\pi \alpha r_o w, \quad (14)$$

conservation of vertical momentum

$$\frac{d[\pi r_o^2 w^2 \rho]}{dz} = \pi r_o^2 g(\rho_a - \rho), \quad (15)$$

and conservation of buoyancy

$$\frac{d[\pi r_o^2 w(\rho_o - \rho)]}{dz} = 2\pi \alpha r_o w(\rho_o - \rho). \quad (16)$$

Equation (14), the conservation of mass equation, states that the vertical divergence of the mass flux at a given height equals the rate of entrainment into the plume at that height. The

left side of Eq. (15) is the vertical rate of change in momentum of the plume and this must be equal to the momentum input due to the buoyancy of the plume. Equation (16) states that the vertical divergence of buoyancy of the plume equals the rate of entrainment of buoyancy into the plume. These equations are solved by using a finite difference scheme in which differences are computed forward in time.

Input variables that drive the model are the density profile of the ambient water column $\rho_o(z)$, and the buoyancy flux b , (Table 3.1.2) of the discharged effluent. Output variables are the plume radius $r(z)$, the equilibrium height h_n where the centerline density of the plume equals that of the ambient waters and the height h_z when the centerline vertical velocity of the plume drops to zero. This one-dimensional model can only describe the initial buoyant rise; it cannot describe the lateral spreading of the plume after its equilibrium level is reached.

As buoyant effluent rises from the diffuser, it continually mixes with ambient waters. In a stratified water column, the mean density of the plume increases until its centerline density reaches the ambient density at a “height of neutral buoyancy” h_n (**Figure 4**). The plume rises beyond h_n because it has upward momentum which carries it into less dense waters above h_n . Soon after, gravity causes the plume to lose this momentum and collapse back upon itself. The height at which the plume vertical momentum goes to zero and the collapse begins is called the height of zero velocity h_v . Eventually the plume settles at a height somewhere between h_n and h_v . The diameter of the plume at h_n allows the prediction of a lower bound on the mean plume dilution (defined as the reciprocal of the concentration of produced water). The dilution of the plume is calculated as the volume of effluent that passes the level of neutral buoyancy divided by the volume discharged from the diffuser. The plume continues to entrain ambient waters during its collapse but the physics involved in this process are poorly understood and difficult to model (Roberts, 1994). The Morton, Taylor, Turner (1956) model is an initial mixing model and is not valid after the plume begins its collapse. After the collapse, the plume establishes a wastefield that is dispersed by ambient currents and further dilution of the plume results from turbulent processes in the surrounding ocean.

FAR FIELD DISPERSION

To predict the biological and ecological impacts of a produced water plume on the local environment, it is necessary to determine both its vertical and horizontal extent. Visitation frequency diagrams (c.f. Csanady, 1983, Roberts, 1986, Roberts, 1989, Roberts and Williams, 1992 for details) of the effluent are constructed from current data to show the dispersion of the wastefield. The value of the visitation frequency at a given location in the area surrounding the diffuser is the total amount of time that the effluent is at a given location normalized by a specified time period of produced water release. To compute a map of visitation frequency, the region of interest is divided into a series of grid lines which specify spatial bins. Progressive displacements due to measured currents are tracked over this binned area. Conceptually one can think of puffs of produced water being released at every current observation and then being tracked along the measured current trajectory over time. The coordinates of each puff are noted after each observation and the amount of time each puff is in a particular bin is summed for that bin. The total time a puff is in each bin is divided by the

time over which effluent is released and the result is the fraction of time the wastefield occupies a given location.

Another useful computation for predicting produced water's impact is to determine the mean concentration of the wastefield at a given location in the far field. This procedure is similar to that of visitation frequency except that the time for effluent to arrive at each bin location is also computed. Using this time, a constant eddy diffusivity model is applied to predict concentration of the puff due to ambient turbulence processes (Brooks, 1960) for every bin. The diffusivity model is applied to a puff starting at the equilibrium height and for the concentration after initial mixing. We used a constant horizontal eddy diffusivity of $K_h = 0.016 \text{ m}^2\text{s}^{-1}$ (Baumgartner *et al.* 1994). This value agrees with values found by Okubo (1980) and Lam *et al.* (1984) for estuaries and coastal waters. When each puff is in a particular bin, the concentration of the puff is added to the running sum of concentrations at within that bin. The summed concentration in every bin is then normalized by the number of times the effluent puffs occupy each bin to give the average concentration of the produced water there over the time period of effluent release. Several factors can cause errors in this approach. One, eddy diffusivities are not constant in space and time and can vary over one to two orders of magnitude. Two, the ambient turbulence that reduces the concentration of effluent in one bin can increase it in the neighboring bins. This dispersion is not accounted for. Three, turbulence is three dimensional and may cause additional vertical spreading besides that which occurs during the plume's initial rise.

SEASONAL EVOLUTION OF THE WATER COLUMN

Time-depth contours derived from temperature profiles show that the year has two distinct thermal regimes: the summer regime, characterized by strong thermal stratification, begins in May and ends around October; and the winter regime, characterized by weak thermal stratification, comprises the rest of the year (**Figure 5a**). Changes in salinity had their major affect on density (**Figure 5b, c**) during rainy periods (**Figure 2a, 2b**). The water column was thermally stratified when our measurements began on 29 July 1992. Cooling began in September, but thermal stratification continued throughout the month. Between 27 September and 24 October stratification in the water column weakened, as the water column warmed to a uniform temperature of 19°C and salinity decreased to 33.2 psu, indicating the advection of a new water mass. From 24 October 1992 until 22 December 1992, the entire water column cooled from 19°C to 13°C raising the density anomaly from 23.8 kg/m³ to 24.6 kg/m³. From 22 December 1992 until summer thermal stratification began in May 1993, the temperature of the water column varied from 13 to 14°C with the exception of a brief warming event in March of 1993 when there was a 0.5- 1.0°C warming of the upper 10 m. In January of 1993, salinity decreased dramatically due to a large input of fresh water from runoff during winter storms. Salinity decreased from 33.0 psu on 22 December 1992 to the lowest salinity observed, 31.4 psu at the surface on 20 January 1993. This resulted in the largest stratification observed when density anomaly varied from 24.2 kg/m³ at the bottom to 23.2 kg/m³ at the surface. A similar fresh water event was observed on 5 March 1993 when the salinity dropped to 32.4 psu at the top of the water column, although stratification during this event was not as

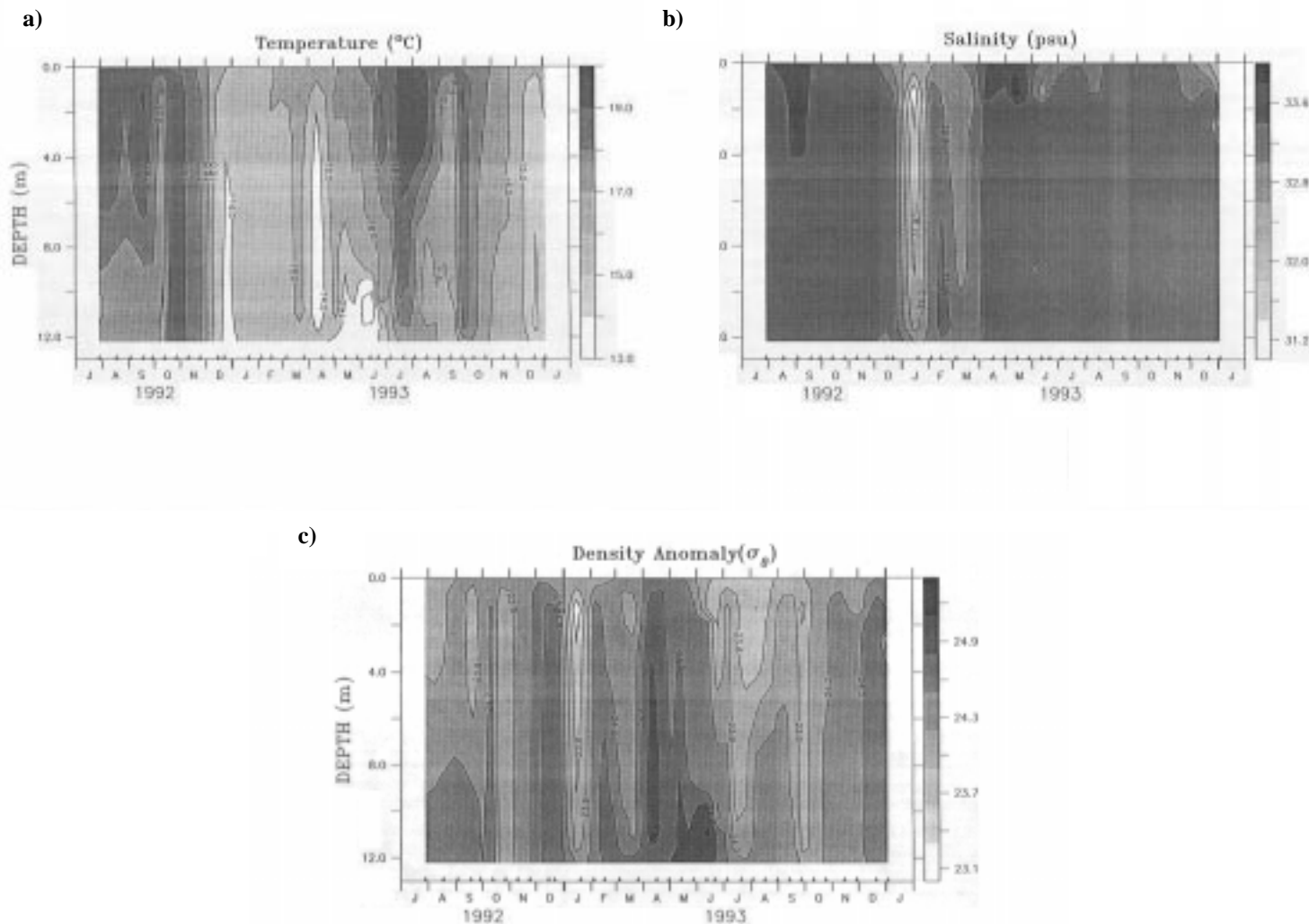


Figure 5. **a)** Contour map of temperature versus depth for the entire data record. Arrows denote times when data is present. The Seabird SBE 19 CTD is unable to record data in the upper 0.5 m of the water column. Due to daily tidal differences, the water column above the diffuser varies from 10.5 to 12.5 m over the period of observation, causing contours to be inaccurate above 0.5 m and below 11 m. **b)** As in **a** except contours are of salinity. **c)** As in **a** except contours are of σ_t where $\sigma_t = \rho - 1000$ and ρ is ambient density in kg/m^3 .

strong as on 20 January 1993. After that event the water column was almost isopycnal until heating began around 30 April 1993 when the upper 2 meters of the water column warmed slightly. On that day, the highest salinity observed (34 psu) occurred at the surface. The maximum thermal stratification observed occurred on 21 June 1993 when the temperature varied from 18.0°C at the surface to 13.0°C at a depth of 10 meters. Sigma-t varied from 24.8 kg/m^3 at the bottom to 23.2 kg/m^3 at the surface. Thermal stratification in 1993 persisted until mid-October. A pattern similar to September 1992 was repeated in August of 1993, when the water column cooled by 1.0°C from the month before. By 25 October, the water column was isothermal with a temperature of 16.5°C . After this the temperature of the water column decreased to 14°C at the bottom and 14.5°C at the surface as the period of observation ended. These observations suggest that the period from October to December is the only time when stratification is consistently weak. This period is after the end of the summertime heating, but is before the wintertime storms. During years of light storm activity, the water column could remain unstratified for the entire period from October until April.

SEASONAL VARIATION OF CURRENTS

Time series of current velocity for stratified conditions (buoyancy frequency $N > 14.5$ cycles hour^{-1} , **Figure 6**) and for weakly stratified conditions (buoyancy frequency $N < 5.5$ cycles hour^{-1} , **Figure 7**) show that currents at 5 m follow isobaths from east to west and vary from 0 to 20 cm s^{-1} in magnitude for both stratifications. The periodic fluctuations in current magnitude for each record indicate that the currents are forced by the semi-diurnal (M2) tide. Shallow water current observations from other locations in the Southern California Bight also show the dominance of the semidiurnal tide. Winant and Olson (1976) reported 10 cm s^{-1} longshore currents due to the M2 tide at 18 m depth in coastal waters off Del Mar California. Power spectra of current magnitude computed using data from 5 July 1993 to 3 January 1994 current data show clear peaks in energy at the diurnal and semidiurnal frequencies (**Figure 8**). Currents 1 m from the bottom are generally weaker and have a greater cross-shelf component than those 5 m above the bottom. Currents for the weakly stratified period show a component that oscillates along shore at the tidal periods overlaid on a mean current. Currents during the strongly stratified period also have a component that oscillates at the tidal periods, but they seem to have a random non-coherent component in the cross shelf direction at both 5 m and 1 m. Internal waves during strongly stratified periods have been reported (Cairns and Nelson (1970), Winant and Olson (1976) and Winant and Bratkovich (1980)) on the Southern California shelf, and may cause this scatter (**Figure 6**). The sampling scheme used for the current measurements in this study is not sufficient to characterize internal waves. Currents during the weakly stratified period lack this random non-coherent component and show little cross shelf flow at 5 m above the bottom.

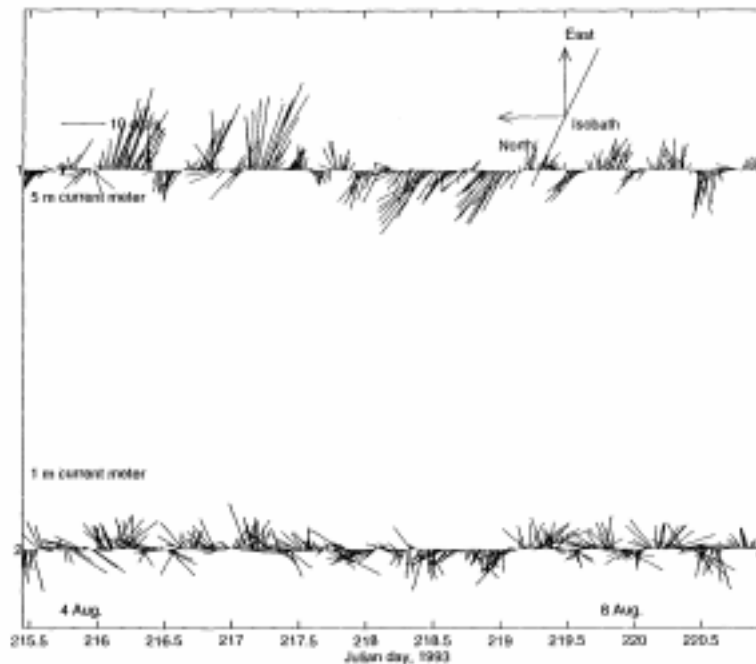


Figure 6. Needle plots of current magnitude and direction. Each needle represents a 2 minute vector average of a current velocity, with each needle 20 minutes apart. The currents are measured at 5 m (upper plot) and at 1 m (lower plot) above the bottom. Vector plots of currents during stratified conditions ($N = 14.5$ cycles sec^{-1}) from 3 August to 9 August 1993.

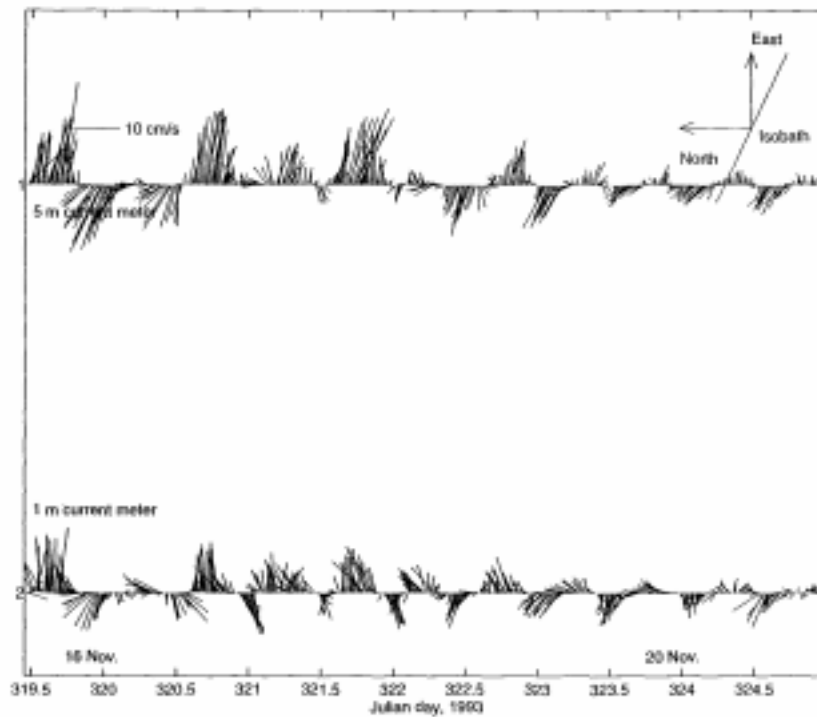


Figure 7. Needle plots of current magnitude and direction (see caption for **Figure 5** for details). Vector plots of currents during unstratified conditions (Buoyancy frequency = 5.5 cycles sec.⁻¹) from 15 November to 21 November 1993.

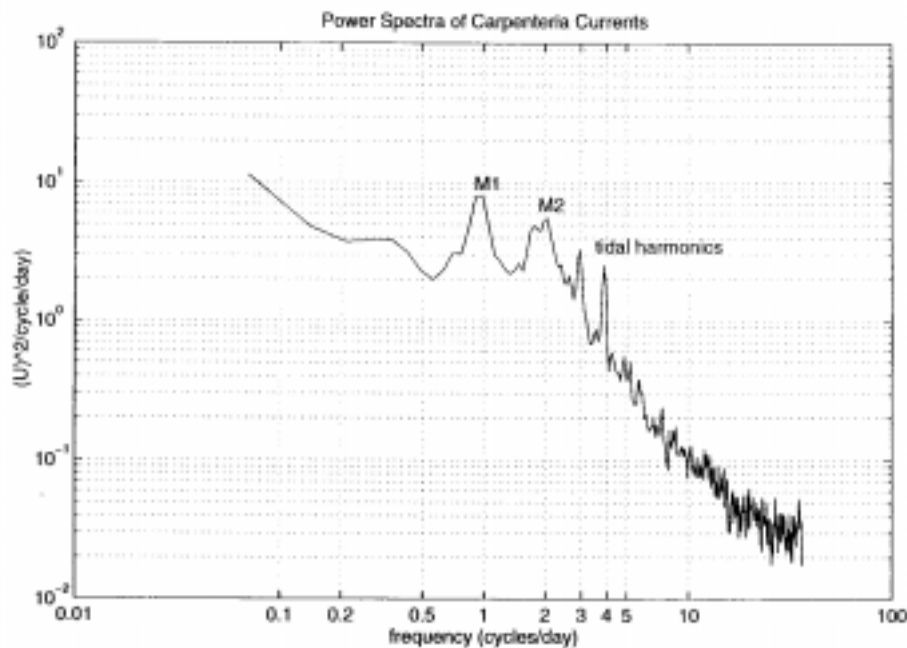


Figure 8. Power spectra of current magnitude for the currents 5 m above the bottom from 5 July 1993 to 3 January 1994. Peaks at 1 cycle and 2 cycles per day, with tidal harmonics at 3 and 4 cycles per day, show considerable energy at tidal frequencies.

To systematically examine current directions, all current data are divided into two groups according to stratification: strongly stratified, $N > 6.0 \text{ cycles hr}^{-1}$, and weakly stratified, $N < 6.0 \text{ cycles hr}^{-1}$. These groups are then sorted into histograms of current direction for strong

stratification (**Figure 9a and b**) and weak stratification (**Figure 10a and b**). The bin width of the histograms is 2 degrees. Histograms for the 5 m (above bottom) currents are similar for both the strongly stratified (**Figure 9a**) and weakly stratified (**Figure 10a**) periods. There are two distinct peaks at 90 degrees (east) and at 270 degrees (west) indicating that most currents flow alongshore, with the currents more frequently flowing to the west. Directional histograms of the 1 m (above bottom) currents are also similar for the strongly stratified (**Figure 9b**) and the weakly stratified (**Figure 10b**) periods, but differ markedly from current histograms at 5 m. Direction histograms at 1 m from the bottom show no clear peaks, but exhibit relatively uniform distributions of current direction. There is a slight increase in the frequency of westward flow for both levels of stratification along with a decrease in frequency of onshore flow. Spikes in all direction histograms at 0°, 90°, 180° and 270° are residual artifacts due to low flow speeds ($\sim 2 \text{ cm s}^{-1}$).

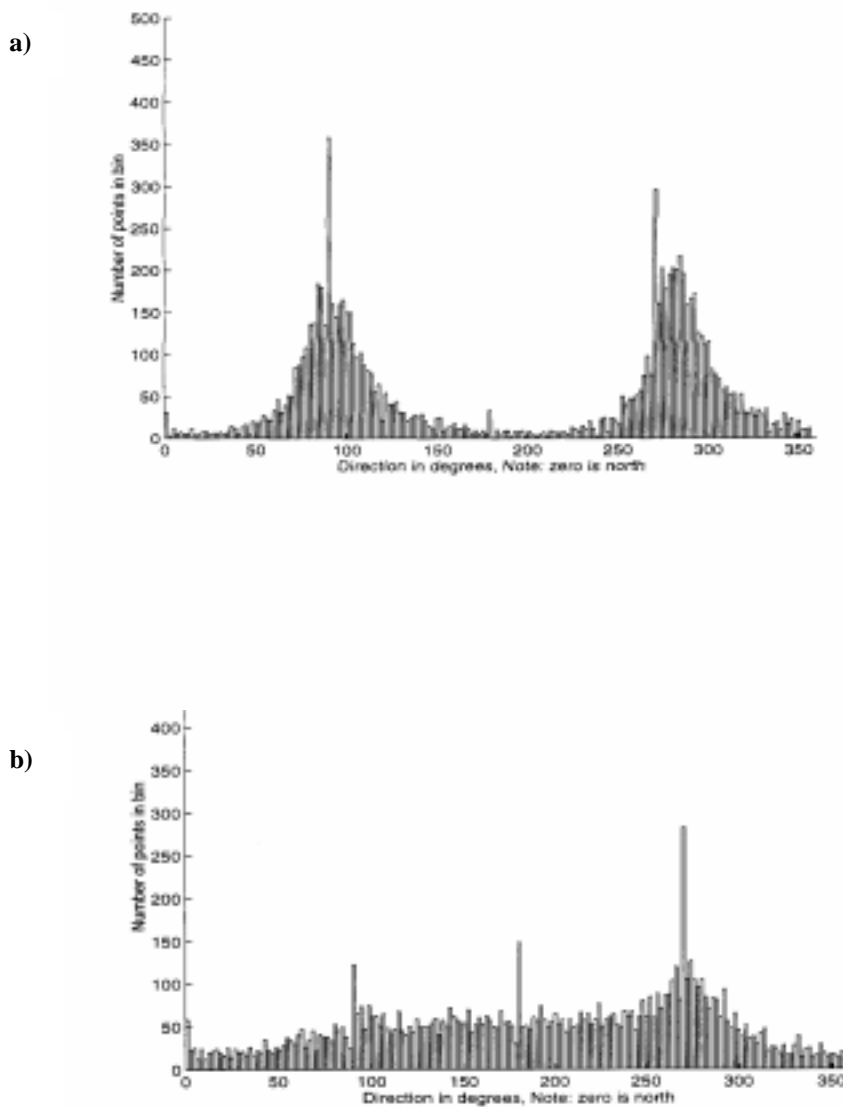


Figure 9. **a)** Histogram of current direction for all stratified periods ($N > 6.0$ cycles per second) for currents measured 5 m from the bottom. Currents with speeds less than 2 cm s^{-1} have been omitted. Peaks in direction at 90 and 270 degrees depict along shore currents. **b)** Same as **a**, except currents were measured 1 m from the bottom.

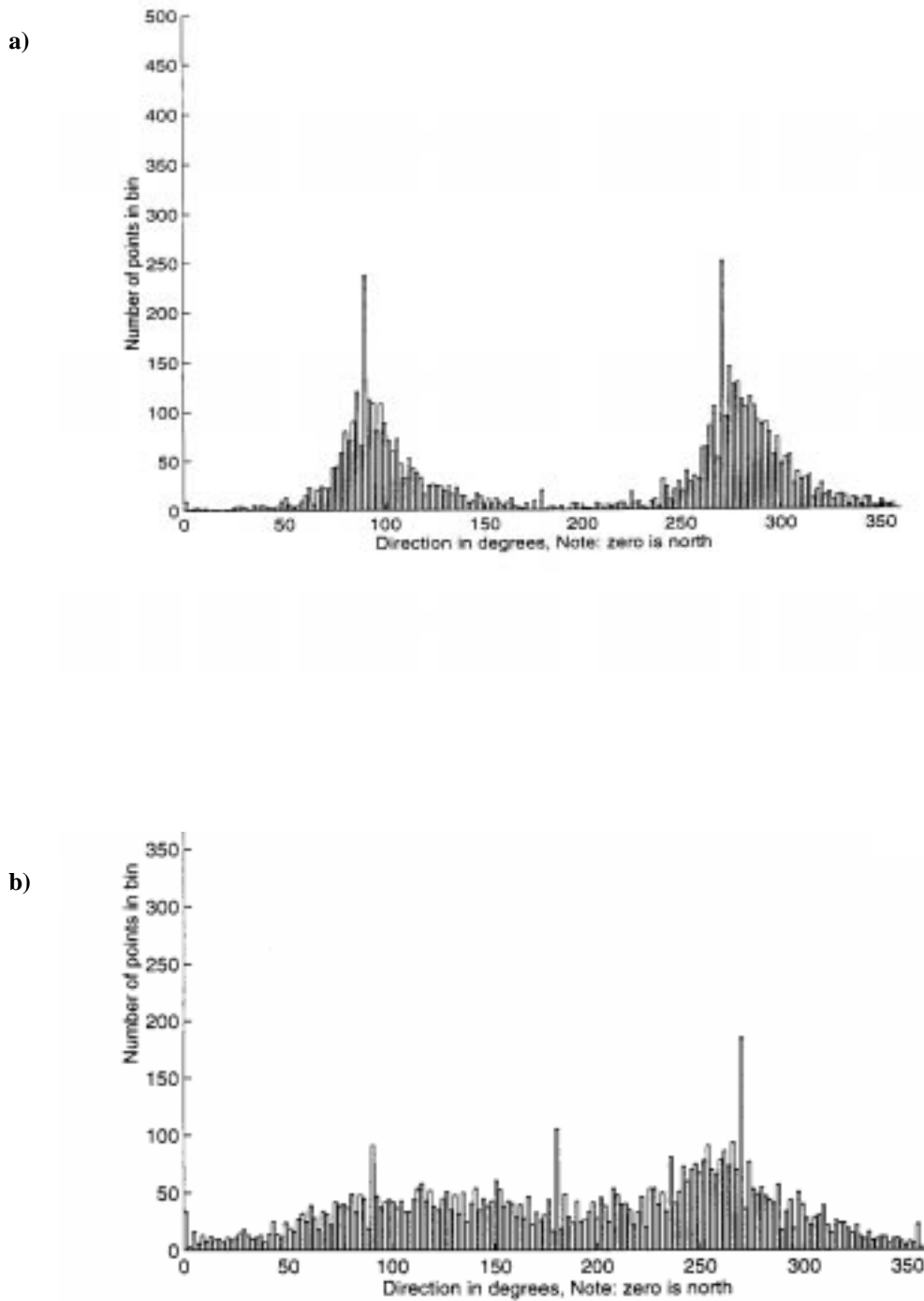


Figure 10. a) Histogram of current direction for all unstratified periods ($N < 6.0$ cycles second⁻¹) for currents measured 5 m from the bottom. b) Same as a, except currents were measured 1 m from the bottom.

MODEL RESULTS

Initial Mixing Models

Calculations to predict the height of the top of the wastefield are made using the Morton, Taylor, Turner (MTT) model and the RSB model. Since the RSB model incorporates ambient currents, two cases were examined, one for ambient current velocities of 1 cm s^{-1} (called RSB1) and the other for velocities of 10 cm s^{-1} (RSB10), in order to span the typical range of

current velocities at the Carpinteria site (**Figures 6 and 7**). The height of the top of the wastefield is plotted over the time-depth contours of density anomaly, for the MTT, RSB1 and RSB10 in **Figure 11**; results from MTT, RSB1 and RSB10 are plotted separately in **Figures 12, 13 and 14** respectively. The model-predicted heights of rise follow the density stratification for all cases such that the wastefield is deeper when stratification is greater. All models predict similar heights for the top of the wastefield. Of the three models, RSB1 predicts the wastefield is highest in the water column for most times, RSB10 generally predicts the lowest with MTT usually in between the other two predictions. Thermal stratification in the summertime caused the plume to remain low in the water column, typically 3 m above the bottom, which is also the height of the mussel outplants (horizontal solid line in **Figures 11, 12, 13 and 14**). The bottom of the wastefield (predicted from RSB1 and RSB10 but not the MTT) during this period is close to the sea floor (~1 m above the bottom). With the breakdown of stratification in the fall, the wastefield rose higher in the water column. Wastefield surfacing should have been common from late October until salinity stratification due to fresh water inputs began. When the plume surfaces under these conditions, RSB1 predicted the bottom of the wastefield would have risen above 3 m. Precipitation in the winter caused the plume to rise and fall through the water column depending upon quantity and timing of the rainfall. For example RSB1 predicted the plume surfaced on 4 February 1993, during a period of weak stratification. Two weeks prior, during a period of strong salinity stratification, the model predicted that the plume was confined below 4 m from the bottom. This up-and-down pattern continued until thermal stratification began around late April.

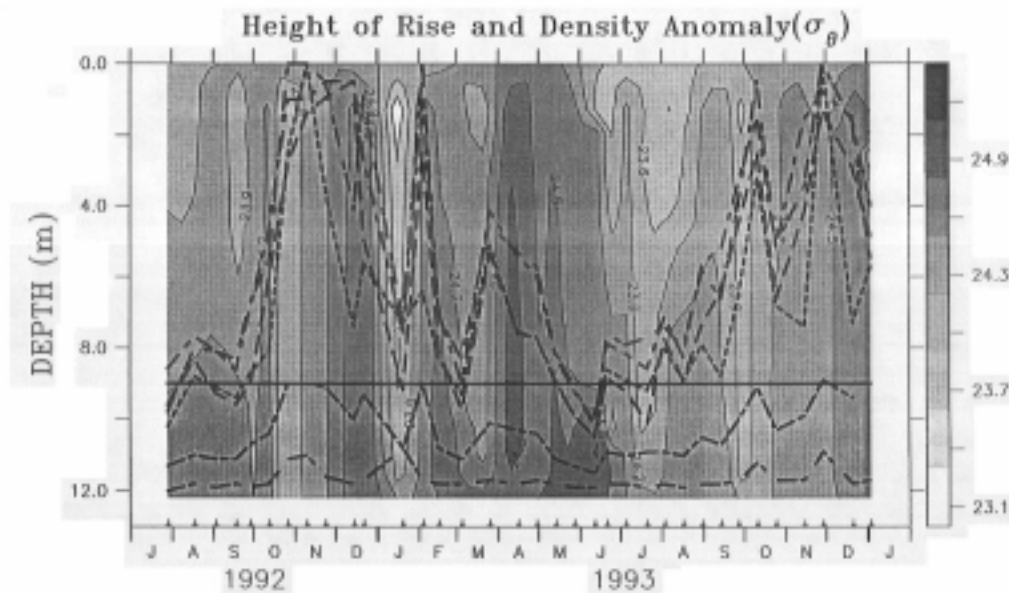


Figure 11. Height of rise for MTT, RSB1 and RSB10 plotted over sigma theta contours (see **Figure 5c**) are: the height of neutral buoyancy (h_n , — —), and the height of zero velocity h_z , (— — —) for the MTT model (see **Figure 4**), the maximum height of rise h_e (— · — ·) and the bottom of the wastefield (— · — ·) for the RSB1 model (see **Figure 4**) and the maximum height of rise h_e (— · — ·) and the bottom of the wastefield (— · — ·) for the RSB10 model (see **Figure 4**). Heights of rise follow density contours throughout the course of the data set. The height of mussel and red abalone outplants (——) are displayed.

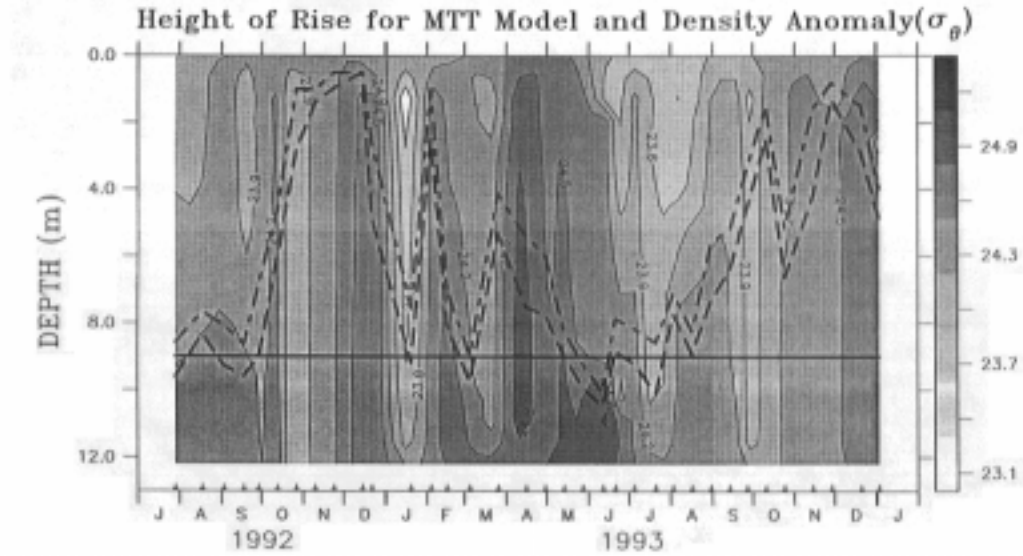


Figure 12. Contours of σ_t with the height of neutral buoyancy h_n (---) and the height of zero velocity h_z (---) for the MTT model (see **Figure 4**).

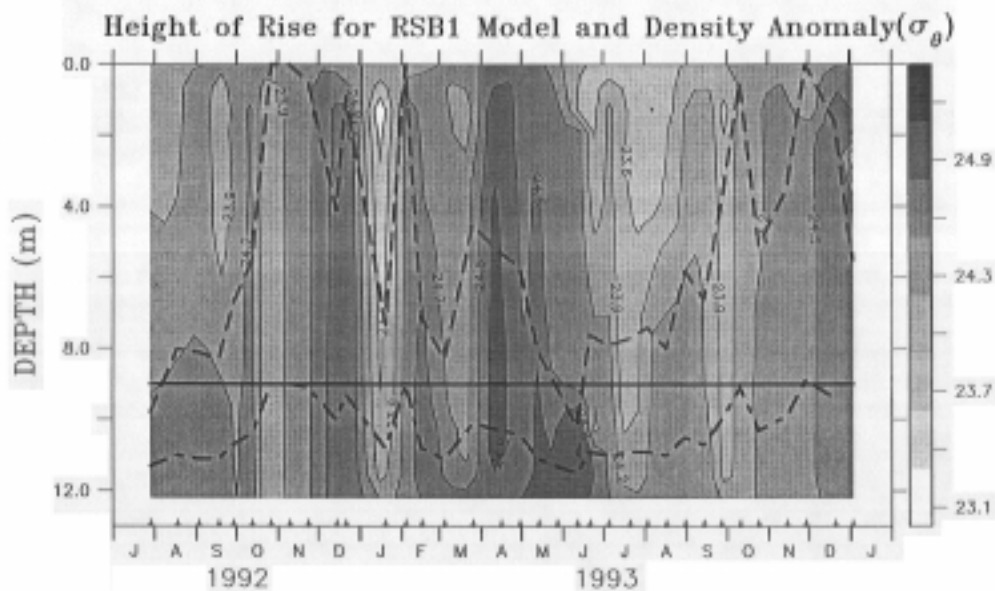


Figure 13. Contours of σ_t with the maximum height of rise h_e (---) and the bottom of the wastefield (---) for the RSB1 model (see **Figure 4**).

In addition to predicting the height of the wastefield, the initial mixing models can predict the dilution of the effluent (**Figure 15**). Dilution of the effluent is closely tied to the height of rise of the plume, since the higher the plume rises, the greater the opportunity for the effluent to mix with ambient water. For the RSB model, predicted initial dilutions are also increased due to ambient current velocity: the more energetic the ambient current, the greater the mixing during plume rise. As a result, RSB1 predicted the least dilution of effluent, with its largest

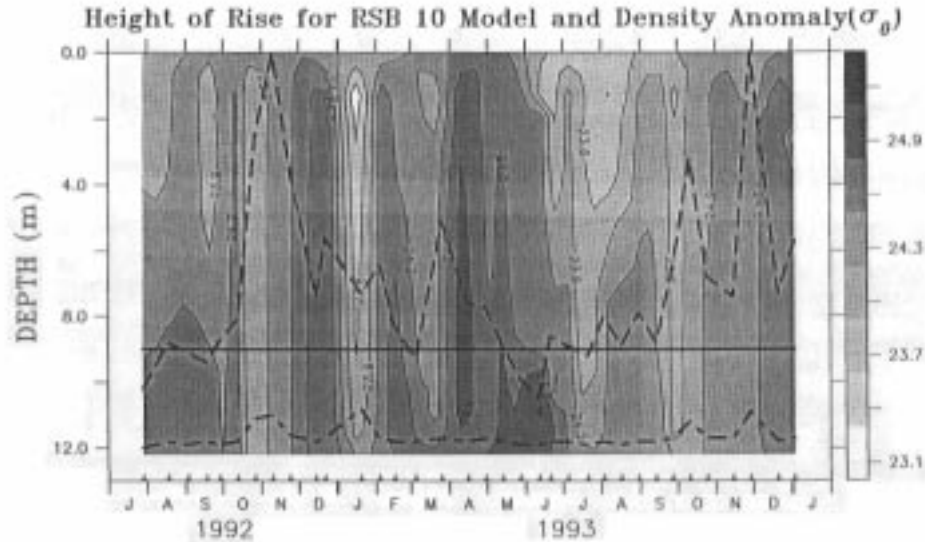


Figure 14. Contours of sigma theta with the maximum height of rise h_c (---) and the bottom of the wastefield (— — —) for the RSB10 model (see Figure 4). The record starts 29 July 1992 and ends 3 January 1994.

predicted dilution being smaller than the lowest dilution predicted by RSB10 even though it predicted a higher height of rise. Estimates of initial dilution of the produced water plume show similar results for the MTT and the RSB10 models, but the RSB1 model predicts dilutions an order of magnitude less. Due to the low buoyancy flux per unit length of the diffuser and the low kinetic energy of the currents, results from the RSB1 model are near the edge of validity of the model (Roberts *et al.*, 1989 a,b,c and Baumgartner *et al.*, 1994). Therefore the dilution results for the RSB1 model are suspect. As expected, the lowest dilutions of effluent are predicted during stratified periods because of the limited height of rise. Typical summertime dilutions are on the order of 1000 - 2000:1 while during periods when the plume surfaces, dilutions increase to around 6000 - 7000:1. The MTT model predicts significantly higher initial dilutions when the plume approaches the surface, because it assumes effluent is always mixing with ambient water. However at some height the plume from each T-port riser will contact the plume from an adjacent riser. At this point the plume will entrain effluent which will cause a general decrease in the initial dilution of the plume. The MTT model cannot predict the decrease in dilution caused by this process while the RSB model takes this process into consideration.

The actual dilution of the effluent plume is probably underestimated because present plume models cannot account for several processes which further increase dilution. No present model of buoyant-jet mixing allows for increased dilution due to the presence of ambient turbulence in the water column during the jet's initial mixing phase (Wright, 1994). Similarly, mixing during the transition from a vertically rising plume to a horizontally spreading wastefield is not understood (Roberts, 1994), and no present models account for this mixing process. Both these factors cause an under-prediction of the initial dilution of the effluent.

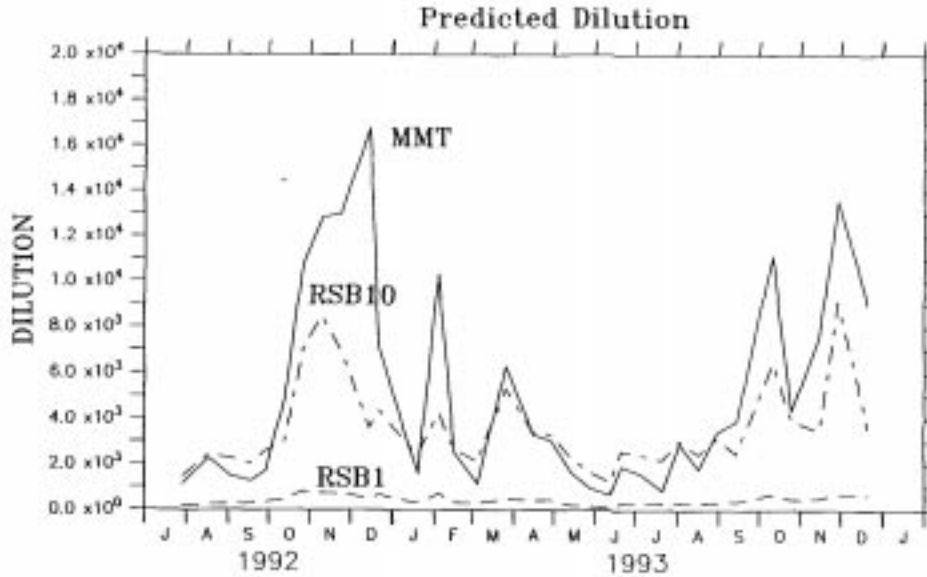


Figure 15. Initial dilution predictions versus Day of Year for MTT (—), RSB1(— · —) and RSB10 (— — —) models. The record starts 29 July 1992 and ends 3 January 1994.

Far Field Dispersion

After the initial mixing of the produced water, only ambient ocean mixing processes cause further dilution of the effluent. As histograms of current direction show, there is little seasonal variation in current direction. Diagrams of visitation frequency for currents 5 m above the bottom (**Figure 16a**) or currents 1 m above the bottom (**Figure 16b**) for periods of high stratification ($N > 6$ cph) are representative of visitation frequency diagrams for any season (data not shown). At 5 m, the currents (**Figure 16a**) would spread effluent along shore with roughly equal spreading in the east and west directions based on the visitation frequency diagram. Whereas at 1 m above the bottom, the wastefield also spreads east to west but is carried primarily offshore.

One of the most important factors in determining the location of the wastefield is the height of rise of the plume. A plume rising high in the water column (unstratified periods) is more likely to be carried along shore. During the more stratified periods when the plume resides lower in the water column the plume is more likely to be carried offshore. Entrainment during the initial mixing phase of the buoyant plume is the primary mechanism responsible for diluting produced water to ambient concentrations. When compared with the entrainment during the buoyant jet phase, entrainment by ambient turbulent processes is slow (Baumgartner *et al.* 1994), even though the ambient current structure at the field site is dynamic and highly variable. As a result, the established wastefield can have high concentrations of produced water and can be highly mobile. Visitation frequency diagrams show that the chances of the wastefield visiting a specific spatial bin close to the diffuser are relatively small. Yet the waste-field retains high concentrations of produced water (over 25% of the concentration of effluent after establishment of the wastefield) at large distances (up to 1 km) from the diffuser. For example, if the plume is located 5 m above the bottom, as is typical in the fall months, produced water is expected farther than 600 m west of the diffuser (outside the 0.01 probability line) up to 10 hours out of every month.

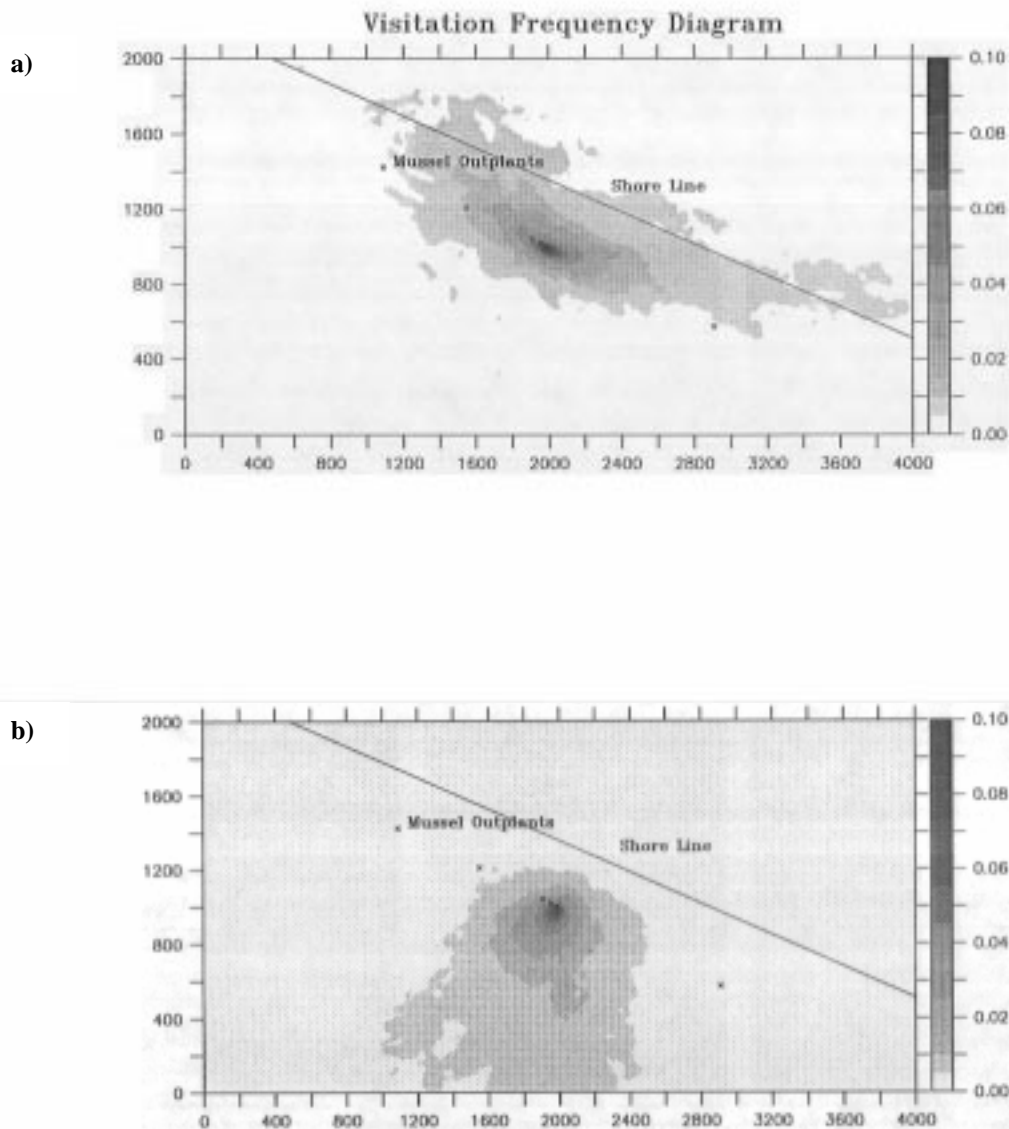


Figure 16. a) Visitation frequency diagrams for the 84 days from 5 July 1993 until 27 September 1993 for a plume located 5 m above the bottom. Contours show percentage defined as the amount of time the plume is in a given location (a 20 m by 20 m bin) normalized by the period of interest (84 days). Each grid point on visitation frequency diagram represents a section 20 m by 20 m (20 points = 400 m). Location of the diffuser is at position (2000, 1000). Lines of constant depth follow the shore line. Mussel outplants used by Krause 1993 are depicted by (x). **b)** As in **a)** except visitation frequency for a plume located 1 m above the bottom.

Relative concentration diagrams (**Figure 17 a,b**) predict the concentration of the effluent for locations around the diffuser, if the wastefield were carried to that location. Contour lines give the concentration of effluent relative to that following initial dilution during plume rise. For example, at a location of 600 m west of the diffuser, effluent concentrations (**Figure 17a**) of 7.0×10^{-5} corresponding to a dilution of 14,000:1 are expected. Krause (1993) established that measurable biological effects occurred when produced water was diluted 10^6 : If the wastefield is low (around 1m) in the water column, as expected in the summer months, produced water will be farther than 600 m to the west of the diffuser less than 1 hour every month (**Figure 16b**). The concentration diagram for the 1 m currents (**Figure 17b**) predicts a higher concentration of 1.0×10^{-4} (dilution of 10,000:1). So, while the effluent does not often

travel far from the diffuser, when it does it may contain large concentrations of produced water, with higher concentrations expected in the more stratified periods.

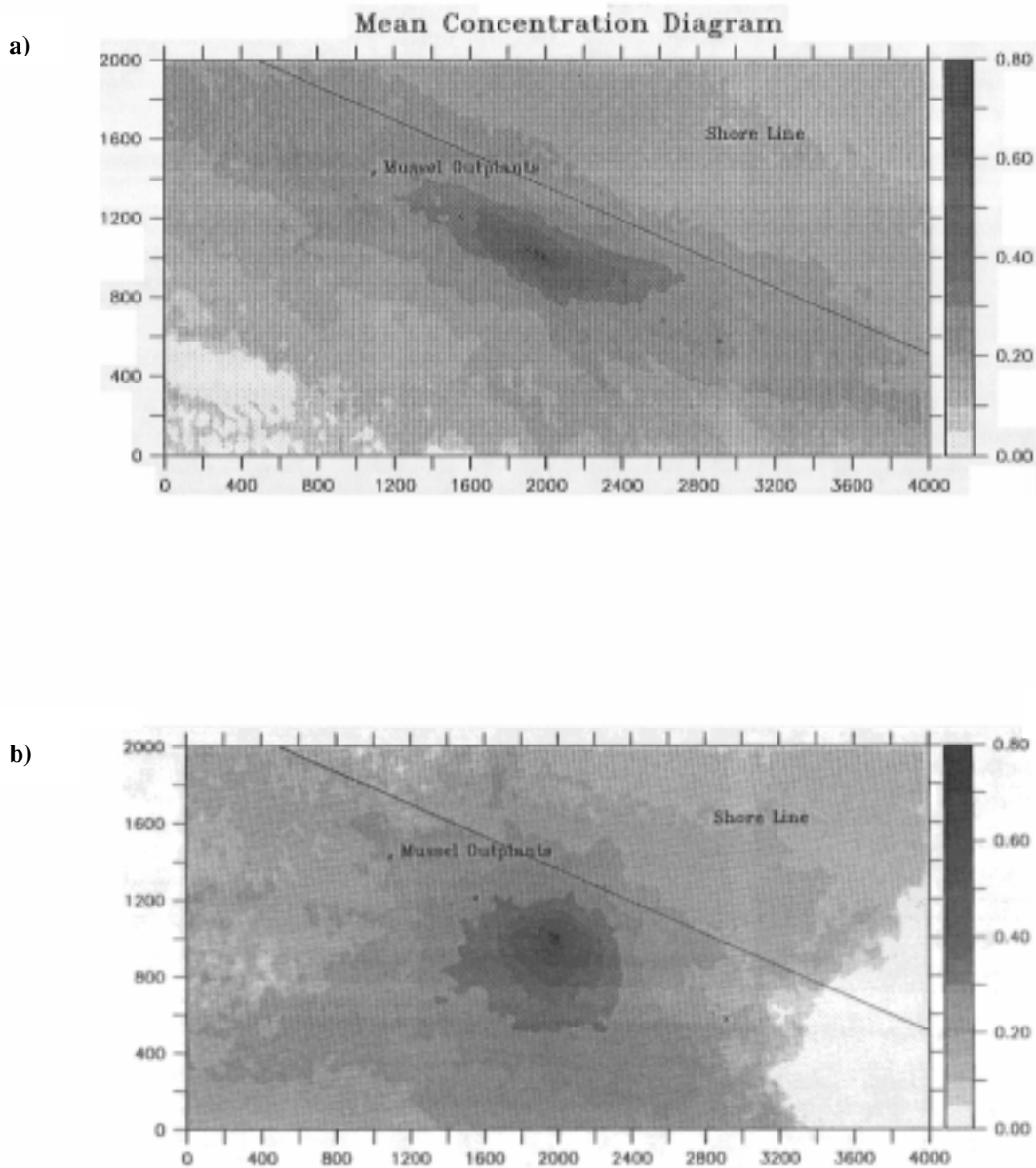


Figure 17. a) Relative concentration diagrams for the period from 5 July until 27 September 1993 calculated for currents 5m from the bottom. Assuming an initial dilution of 1000 to 1 of the discharged produced water, we used a constant eddy diffusivity model (Baumgartner, Frick and Roberts 1994) to calculate the horizontal dilution of the wastefield as it is carried by ambient currents. An eddy diffusivity k_h of $0.0157 \text{ m}^2 \text{ s}^{-1}$ was assumed. Each grid point on the relative concentration diagram represents a section 20 m by 20 m (20 points = 400 m). Location of the diffuser is at position (2000, 1000). Lines of constant depth follow the shore line. Mussel outplants used by Krause 1993 are depicted by (x). **b)** As in **a)** except, relative concentration diagram calculated for currents at 1 m above the bottom.

Visitation frequency diagrams may underestimate the amount of time that the wastefield is located in a particular bin. We assumed that the current field does not vary spatially over the region and that the current field is effectively ‘frozen’. However, the wastefield is over 10 m wide at the diffuser and will occupy several bins at once. In addition, the wastefield is a continuous stream of effluent not a puff. A puff may pass through several spatial bins during a current record and will only be counted in the bin it is located in it at the end of a current record.

While visitation frequency diagrams may underestimate the time of exposure to effluent, relative concentration diagrams may overestimate the concentration because not all mixing processes are accounted for. A simple horizontal eddy diffusivity model is used to estimate the dilution of the wastefield while vertical turbulent diffusion is ignored. Comparison of the current field at 1 m and 5 m above the bottom (**Figures 16 a,b** and **17 a,b**) suggests that shear dispersion may also be important in diluting effluent.

COMPARISON WITH BIOLOGICAL DATA

By combining near-field dilution models with far field dispersion, the duration of exposure of an organism can be predicted and conservative estimates of the concentration of produced water exposure can be made. Seasonal stratification causes the height of rise of the plume to vary which in turn should lead to a seasonal variation in ecological impact. In weakly stratified periods, an increase in the height of rise of the plume causes the initial dilution to increase and currents higher in the water column should carry the wastefield along shore. During strongly stratified periods the opposite occurs: the plume does not rise as high and is therefore not as dilute when deeper, weaker currents carry the plume offshore.

In two separate experiments Raimondi and Schmitt (1992) measured the effects of produced water on red abalone. In the first experiment abalone larvae were moored at 5, 10, 50, 100, 500 and 1000 m west of the diffuser as well as at 5 and 1000 m east of the diffuser at depths of 1.5 m above the bottom and 1.5 m below the surface. The exposure time was 5.5 hours so that short term effects of produced water on larvae survivorship and settlement could be examined. To test the effects of long term exposure to produced water, larvae were outplanted for 4 days at the same locations. Less than 50 m from the diffuser, the long term experiment showed low rates of relative viability, the proportion of larvae that completed the planktonic stage. No effects were observed 1000 m from the diffuser in either direction. The lowest viability reported, 15 %, was 5 m east of the diffuser; 30 % viability occurred 5 m west of the diffuser. Red abalone larvae were subjected to known concentrations of produced water and settlement rates were determined after 24 hour exposures. Exposure to 0.1- 1 percent produced water for 24 hours produced similar settlement rates as seen at the 100 m mooring for the 4 day outplant.

Similar effects were reported by Osenberg *et al.* (1992) who studied the effects of produced water on mussel populations. They outplanted mussel populations 1, 5, 10, 50, 100 and 1000 m to the west of the diffuser at 4.5 m from the bottom from 7 June to 4 October 1990. They found that the tissue production of mussel outplants decreased with proximity to the diffuser, indicating lower relative mussel performance with exposure to produced water. In addition,

they also reported that mussels closer to the produced water diffuser had markedly less gonadal mass, which would decrease their chances of reproductive success.

Krause (1993) collected samples of seawater 1 m above the bottom at 1, 5, 10, 15, 20, 30, 40, 100 and 1000 m west of the diffuser and 1000 m east of the diffuser on 13 May 1992. The fertilization success of purple sea urchins was measured after exposure to these seawater samples. In a separate experiment the reproductive success of purple sea urchins was measured after exposure to known concentrations of produced water. From these, a one-dimensional plume map of concentration versus distance for the Carpinteria site was constructed from data obtained on 13 May 1992. Krause (1993) measured concentrations ranging from 1 part per hundred at 5 m west of the diffuser to 2 parts per million at 1000 m west of the diffuser, as determined from the reproductive success of purple sea urchin. No effluent was detected at 1000 m to the east of the diffuser based on the biological measurement. Current measurements on 13 May 1992 are unavailable making it impossible to make accurate predictions of far field concentrations. The far field dispersion model predicts that the wastefield will occupy the mussel outplant location 1000 m west of the diffuser for only 2 hours out of every month. As a result it is highly unlikely that the effluent wastefield was measured during the 13 May 1992 experiment. Due to the strong M2 tidal component, currents change direction from east to west about every 12 hours allowing the wastefield to be carried back and forth as the current direction changes. This motion may result in the creation of detectable levels of effluent in the ambient water column around the diffuser. Krause reported concentrations of 0.001 percent produced water at 100 m west, compared to the 0.1 to 1 percent concentrations seen by Raimondi and Schmitt (1992). Both Osenberg *et al.* (1992) and Raimondi and Schmitt (1992) found that the effects of produced water decrease with distance from the diffuser for outplants of mussels and red abalone larvae, respectively, for longer exposures. Both studies reported a cessation of effects 1000 m west of the diffuser suggesting a limit to the length scale associated with this ambient concentrations of produced water.

The dynamical nature of the water column makes it difficult to predict the wastefield location and concentration of effluent. The visitation frequency and mean concentration diagrams lend themselves to estimating long term integrative exposure of effluent. Unless current and stratification data are available exact comparison with studies performed by Raimondi and Schmitt (1992), Osenberg *et al.* (1992) and Krause (1993) is impossible. Of the three studies, only Osenberg has temporal scales long enough for it to be likely that the mussels were directly exposed to the effluent wastefield. Only Krause estimates the concentration of produced water to which the purple sea urchins were exposed.

Osenberg's (1992) experimental outplantings of mussels indicated that effects of the plume could be noted as far as 0.5 km whereas effects were only noted as far as 0.1 km for benthic infauna. Waters with a similar dilution to that at the outplantings at 0.5 km were restricted to a band 0.8 km to the west, 0.5 km to the east, and 0.15 km inshore and offshore of the diffuser based on the current velocities 5 m above the bottom. The impacted region was more extensive based on the current velocities 1 m above the bottom. It would have been somewhat elliptical in shape, extending 1 km offshore, 0.7 km west and 0.5 to 1.1 km east of the diffuser. The area in which benthic infauna were affected was 0.038 km².

The plume affected growth rates and production of gonadal mass in the mussels (Osenberg 1992), both of which depend on integrated exposure time to produced water. However, experiments with planktonic larvae (Raimondi and Schmidt, 1992) and purple sea urchins (Krause, 1993) indicated that short exposures to produced water could affect fertilization success, larval survivorship and settlement, and relative viability. Our calculations of visitation frequency, the length of time that the plume spent at any given location, indicated that the plume could reside for hours at distances of several km outside the region causing integrated affects on mussels. These sporadic excursions of plume water intermittently will affect survivorship of larvae of a variety of species up to several km from the diffuser.

CONCLUSIONS

We performed a combined field and modeling study to investigate the dispersion of produced water and its biological consequences. Radiant heating in the summertime caused thermal stratification of the water column from late April until early October. Buoyancy frequencies of 8.0 to 14.0 cycles per hour were observed during these months. For the rest of the year the water column was nearly isothermal. Runoff due to wintertime storm activity caused haline stratification as strong as the thermal stratification observed during summer months. During the fall, from October until rain events started, the water column was weakly stratified with buoyancy frequencies below 5.5 cycles per hour. Current data were taken at two different heights 25 m west of the diffuser. Power spectra of the magnitude of currents at 5 m from the bottom showed that the currents contained strong M1 and M2 tidal components. Currents at 5 m flowed mostly in the long shore direction and currents at 1 m above the bottom have both off shore and along shore components.

Over the course of a year, both thermal and salinity stratification cause the modeled produced water plume to remain low in the water column for about 7 to 8 months and reduced the initial mixing of the effluent with ambient waters. Further mixing of the produced water, due to ambient turbulence in the water column, may not reduce pollutant concentrations below 1 part in a million for up to 72 hours after release during which time the wastefield may be carried 10 km from the diffuser. However, visitation frequency diagrams show the possibility of effluent occupying specific locations this far from the diffuser is extremely low. Krause (1993) developed a field assay of dilution with distance from the diffuser by collecting water samples at increasing distances from the diffuser and measuring fertilization. Our time series of current velocities and density stratification show that the behavior of the wastefield is quite complex and cannot be reliably quantified by this method. Results from field tests by Krause (1993), Osenberg *et al.* (1992) and Raimondi and Schmitt (1992) show a decrease of effluent effects until there are almost no impacts 1000 m west of the diffuser. Our visitation diagrams show that the concentrated wastefield is at this position less than 2 hours every month, indicating only sporadic effects on physiological processes that can be affected by short exposures to produced water. However, based on the experiments with mussels and our relative concentration diagrams, the area in which integrated affects on organisms living in the upper part of the water column would be expected was at least 0.4 km² during the unstratified period. For organisms living lower in the water column, the area in which negative impacts are expected for benthic infauna extends 0.038 km² but for mussels extends at least 1.5 km².

REFERENCES

- Angelidis, P.B. and N.E. Kotsovinos. 1994. The Plane Submerged Horizontal Buoyant Jet. In: *Recent Research Advances in the Fluid Mechanics of Turbulent Jets and Plumes*, P.A. Davies and M.J. Valente Neves, eds. Kluwer Academic, Boston. pp. 29-43
- Baumgartner, D.J., W.E. Frick, and P.J.W. Roberts. 1994. Dilution Models for Effluent Discharges. Document No. N268. Environmental Research Laboratory.
- Brooks, N.H. 1960. Diffusion of Sewage Effluent in an Ocean Current. *Proc. Int. Conf. Waste Disposal Mar. Environ., 1st*. pp. 246-267.
- Cairns, J. L. and K.W. Nelson. 1970. A Description of the Seasonal Thermocline Cycle in Shallow Coastal Water. *J. Geophysical Res.* **75**:1127-1131.
- Csanady, G.T. 1983. Dispersal by Randomly Varying Currents. *J. Fluid Mech.* **132**:375-394.
- Fischer, H.B., E.J. List, R.C.Y. Koh, J. Imberger, and N.H. Brooks. 1979. *Mixing in Inland and Coastal Waters*. Academic Press. New York. 483 p.
- Fofonoff, N.P. and R.C. Millard, Jr. 1983. Algorithms for computation of fundamental properties of seawater *UNESCO technical papers in marine science* #44.
- Higashi, R., G. Cherr, C. Bergens, T. Fan and D. Crosby. 1992. Toxicant Isolation from a Produced Water Source in the Santa Barbara Channel. In: *Produced Water: Technological/Environmental Issues and Solutions*. J.P. Ray and F.R. Engelhardt, eds. Plenum Press, New York. pp. 223-234.
- Interocean Inc. of San Diego, Ca. 1990. Model S4 User's Manual.
- Keough, M.J. and K.P. Black. 1996. Predicting the Scale of Marine Impacts: Understanding Planktonic Links Between Populations . *Detecting Ecological Impacts: Concepts and Applications in Coastal Habitats*. R.J. Schmitt and C.W. Osenberg, eds. Academic Press, San Diego, CA. pp. 199-234.
- Kotsovinos, N.E. and E.J. List. 1977. Plane turbulent Buoyant Jets. Part 1. Integral Properties. *J. Fluid Mechanics* **81**:25-44.
- Krause, P.R., C.W. Osenberg, and R.J. Schmitt. 1992. Effects of Produced Water on Early Life Stages of a Sea Urchin: Stage-Specific Responses and Delayed Expression. In: *Produced Water: Technological/Environmental Issues and Solutions*. J.P. Ray and F.R. Engelhardt, eds. Plenum Press, New York. pp. 431-444.
- Krause, P. 1993. *Effects of Produced Water on Reproduction and Early Life Stages of the Purple Sea Urchin (*Strongylocentrotus purpuratus*): Field and Laboratory Tests*. Ph.D. Dissertation. University of California, Santa Barbara. xx 140.
- Lam, D.C.L., C.R. Murthy, and R.B. Simpson. 1984. *Effluent Transport and Diffusion Models for the Coastal Zone*. Lec. Notes on Coastal and Estuarine Studies, #5. Springer-Verlag, New York. 168 p.
- Morton, B.R., G.I. Taylor and J.S. Turner. 1956. Turbulent gravitational convection from maintained and instantaneous sources. *Proc. Roy. Soc.* **A234**:1-23.
- Okubo, A. 1980. *Diffusion and Ecological Problems: Mathematical Models*. Springer-Verlag, New York. 254 p.

- Osenberg, C.W., R.J. Schmitt, S.J. Holbrook, and D. Canestro. 1992. Spatial Scale of Ecological Effects Associated with an Open Coast Discharge of Produced Water. In: *Produced Water: Technological/Environmental Issues and Solutions*. J.P. Ray and F.R. Engelhardt, eds. Plenum Press, New York. pp. 387-402.
- Raimondi, P.T. and R.J. Schmitt. 1992. Effects of Produced Water on Settlement of Larvae: Field Tests Using Red Abalone. In: *Produced Water: Technological/Environmental Issues and Solutions*. J.P. Ray and F.R. Engelhardt, eds. Plenum Press, New York. pp. 415-430.
- Roberts, Philip J.W. 1986. The Use of Current Data in Ocean Outfall Design. *Wat. Sci. Tech.* **18**:111-120.
- Roberts, Philip J.W. 1989. Dilution and Transport Predictions for Ocean Outfalls. *Wat. Sci. Tech.* **21**:969-979.
- Roberts, P.J.W., W.H. Snyder, and D.J. Baumgartner. 1989. Ocean Outfalls. I: Submerged Wastefield Formation. *J. Hydraulic Engineering* **115**:1-25.
- Roberts, P.J.W., W.H. Snyder, and D.J. Baumgartner. 1989. Ocean Outfalls. II: Spatial Evolution of Submerged Wastefield. *J. Hydraulic Engineering* **115**:26-48.
- Roberts, P.J.W., W.H. Snyder, and D.J. Baumgartner. 1989. Ocean Outfalls. III: Effect of Diffuser Design on Submerged Wastefield. *J. Hydraulic Engineering* **115**:49-70.
- Roberts, P.J.W. and N. Williams. 1992. Modeling of Ocean Outfall Discharges. *Wat. Sci. Tech.* **25**:155-164.
- Roberts, P.J.W. 1994. Jets and Plumes and Ocean Outfall Design. In: *Recent Research Advances in the Fluid Mechanics of Turbulent Jets and Plumes*, P.A. Davies and M.J. Valente Neves, eds. Kluwer Academic, Boston. pp. 441-464.
- Turner, J.S. 1986. Turbulent Entrainment: the Development of the Entrainment Assumption, and its Application to Geophysical Flows. *J. Fluid Mechanics* **173**:431-471.
- Winant, C.D. and J.R. Olson. 1976. The vertical structure of coastal currents. *Journal of Deep Sea Research* **23**:925-936.
- Winant, C.D. and A.W. Bratkovich. 1980. Temperature and Currents on the Southern California Shelf: A Description of Variability. *Journal of Physical Oceanography* **11**:71-86.
- Wright, S.J. 1994. The Effect of Ambient Turbulence on Jet Mixing. In: *Recent Research Advances in the Fluid Mechanics of Turbulent Jets and Plumes*, P.A. Davies and M.J. Valente Neves, eds. Kluwer Academic, Boston. pp. 13-27.
- Wu, Yicun. 1993. The Study of an Ocean Outfall Buoyant Plume Near Whites Point, California. *Ph.D Dissertation*, University of Southern California.
- Wu, Y., L. Washburn and B.H. Jones. 1994. Buoyant Plume Dispersion in a Coastal Environment: Evolving Plume Structure and Dynamics. *Continental Shelf Research* **14**:1001-1023.



The Department of the Interior Mission

As the Nation's principal conservation agency, the Department of the Interior has responsibility for most of our nationally owned public lands and natural resources. This includes fostering sound use of our land and water resources; protecting our fish, wildlife, and biological diversity; preserving the environmental and cultural values of our national parks and historical places; and providing for the enjoyment of life through outdoor recreation. The Department assesses our energy and mineral resources and works to ensure that their development is in the best interests of all our people by encouraging stewardship and citizen participation in their care. The Department also has a major responsibility for American Indian reservation communities and for people who live in island territories under U.S. administration.



The Minerals Management Service Mission

As a bureau of the Department of the Interior, the Minerals Management Service's (MMS) primary responsibilities are to manage the mineral resources located on the Nation's Outer Continental Shelf (OCS), collect revenue from the Federal OCS and onshore Federal and Indian lands, and distribute those revenues.

Moreover, in working to meet its responsibilities, the **Offshore Minerals Management Program** administers the OCS competitive leasing program and oversees the safe and environmentally sound exploration and production of our Nation's offshore natural gas, oil and other mineral resources. The **MMS Royalty Management Program** meets its responsibilities by ensuring the efficient, timely and accurate collection and disbursement of revenue from mineral leasing and production due to Indian tribes and allottees, States and the U.S. Treasury.

The MMS strives to fulfill its responsibilities through the general guiding principles of: (1) being responsive to the public's concerns and interests by maintaining a dialogue with all potentially affected parties and (2) carrying out its programs with an emphasis on working to enhance the quality of life for all Americans by lending MMS assistance and expertise to economic development and environmental protection.